



Transportation Consortium of South-Central States

*Solving Emerging Transportation Resiliency, Sustainability, and Economic Challenges through the Use of Innovative Materials and Construction Methods: From Research to Implementation*

# **Elimination of Empirical, Ineffective and Expensive PG Plus Tests to Characterize Modified Binders**

Project No. 18BASU02

Lead University: Arkansas State University

**Final Report  
August 2019**

### **Disclaimer**

The contents of this report reflect the views of the authors, who are responsible for the facts and the accuracy of the information presented herein. This document is disseminated in the interest of information exchange. The report is funded, partially or entirely, by a grant from the U.S. Department of Transportation's University Transportation Centers Program. However, the U.S. Government assumes no liability for the contents or use thereof.

### **Acknowledgements**

The authors acknowledge the Tran-SET for providing the financial support of this study. The authors also would like to thank Ergon, Inc., Memphis, TN for providing test materials for this study. Special thanks to Dr. Hashim Ali and Mr. Kotaiba Abugazleh for their help with FTIR tests.

## TECHNICAL DOCUMENTATION PAGE

<b>1. Project No.</b> 18BASU02	<b>2. Government Accession No.</b>	<b>3. Recipient's Catalog No.</b>	
<b>4. Title and Subtitle</b>  Elimination of Empirical, Ineffective and Expensive PG Plus Tests to Characterize Modified Binders		<b>5. Report Date</b> Aug. 2019	
<b>7. Author(s)</b> PI: Zahid Hossain <a href="https://orcid.org/0000-0003-3395-564X">https://orcid.org/0000-0003-3395-564X</a> Co-PI: Ashraf Elsayed <a href="https://orcid.org/0000-0003-1506-2784">https://orcid.org/0000-0003-1506-2784</a> GRA: MM Tariq Morshed <a href="https://orcid.org/0000-0002-2299-7011">https://orcid.org/0000-0002-2299-7011</a> GRA: Mohammad N. Hassan <a href="https://orcid.org/0000-0003-3583-3101">https://orcid.org/0000-0003-3583-3101</a>		<b>6. Performing Organization Code</b>	
<b>9. Performing Organization Name and Address</b> Transportation Consortium of South-Central States (Tran-SET) University Transportation Center for Region 6 3319 Patrick F. Taylor Hall, Louisiana State University, Baton Rouge, LA 70803		<b>8. Performing Organization Report No.</b>	
<b>12. Sponsoring Agency Name and Address</b> United States of America Department of Transportation Research and Innovative Technology Administration		<b>10. Work Unit No. (TRAIS)</b>	
<b>15. Supplementary Notes</b> Report uploaded and accessible at <a href="http://transet.lsu.edu/">Tran-SET's website (http://transet.lsu.edu/)</a>		<b>11. Contract or Grant No.</b> 69A3551747106	
<b>16. Abstract</b> For characterizing the polymer modified binders, different state Departments of Transportation (DOTs) use different time consuming and empirical Performance Grade (PG) Plus test methods. Furthermore, the PG Plus tests are silent when asphalt binders are modified with chemicals such as polyphosphoric acid (PPA). But, the effects of the elastomeric or plastomeric polymer are not accurately identified through these conventional tests such as Elastic Recovery (ER) and tenacity. Thus, the main research goal of this study is to recommend alternative test method(s), which can possibly be pursued by using a commonly available device, a Dynamic Shear Rheometer (DSR). Three PG binders (PG 64-22, PG 70-22 and PG 76-22) certified in Arkansas have been selected for this investigation. These asphalt binders from different sources were evaluated in the laboratory to establish a good correlation. These binders have been prepared with different modifiers: styrene-butadiene-styrene (SBS) polymer, PPA, or a combination of both. Multiple Stress Creep and Recovery (MSCR), ER-DSR, Linear Amplitude Sweep (LAS), and Binder Yield Energy Test (BYET) were explored to find their effectiveness. After exploring the DSR-based tests, it can be concluded that the ER-DSR and MSCR tests can be good replacements of elastic recovery test (AASHTO T 301). However, the presence of PPA cannot be identified by following these test methods. Thus, chemical tests such as SARA (Saturate, Aromatic, Resin and Asphaltene) analysis, pH and FTIR (Fourier-transform Infrared spectroscopy) were explored to identify the presence of PPA. The pH measurement test was found to be useful to trace the presence of acid and degree of modification. The SARA analysis was used for observing the changes in chemical fraction due to aging and subsequently useful to predict rutting. On the other hand, spectroscopical analysis (FTIR) was found to be an effective tool to evaluate the change in chemical fingerprint due to aging.		<b>13. Type of Report and Period Covered</b> Final Research Report Mar. 2018 – Mar. 2019	
<b>17. Key Words</b> PG Plus binder, Elastic Recovery (ER), MSCR, ER-DSR, FTIR, pH		<b>14. Sponsoring Agency Code</b>	
<b>18. Distribution Statement</b> No restrictions. This document is available through the National Technical Information Service, Springfield, VA 22161.		<b>15. Supplementary Notes</b>	
<b>19. Security Classif. (of this report)</b> Unclassified	<b>20. Security Classif. (of this page)</b> Unclassified	<b>21. No. of Pages</b> 46	<b>22. Price</b>

Form DOT F 1700.7 (8-72)

Reproduction of completed page authorized.

## SI\* (MODERN METRIC) CONVERSION FACTORS

### APPROXIMATE CONVERSIONS TO SI UNITS

Symbol	When You Know	Multiply By	To Find	Symbol
<b>LENGTH</b>				
in	inches	25.4	millimeters	mm
ft	feet	0.305	meters	m
yd	yards	0.914	meters	m
mi	miles	1.61	kilometers	km
<b>AREA</b>				
in <sup>2</sup>	square inches	645.2	square millimeters	mm <sup>2</sup>
ft <sup>2</sup>	square feet	0.093	square meters	m <sup>2</sup>
yd <sup>2</sup>	square yard	0.836	square meters	m <sup>2</sup>
ac	acres	0.405	hectares	ha
mi <sup>2</sup>	square miles	2.59	square kilometers	km <sup>2</sup>
<b>VOLUME</b>				
fl oz	fluid ounces	29.57	milliliters	mL
gal	gallons	3.785	liters	L
ft <sup>3</sup>	cubic feet	0.028	cubic meters	m <sup>3</sup>
yd <sup>3</sup>	cubic yards	0.765	cubic meters	m <sup>3</sup>
NOTE: volumes greater than 1000 L shall be shown in m <sup>3</sup>				
<b>MASS</b>				
oz	ounces	28.35	grams	g
lb	pounds	0.454	kilograms	kg
T	short tons (2000 lb)	0.907	megagrams (or "metric ton")	Mg (or "t")
<b>TEMPERATURE (exact degrees)</b>				
°F	Fahrenheit	5 (F-32)/9 or (F-32)/1.8	Celsius	°C
<b>ILLUMINATION</b>				
fc	foot-candles	10.76	lux	lx
fl	foot-Lamberts	3.426	candela/m <sup>2</sup>	cd/m <sup>2</sup>
<b>FORCE and PRESSURE or STRESS</b>				
lbf	poundforce	4.45	newtons	N
lbf/in <sup>2</sup>	poundforce per square inch	6.89	kilopascals	kPa
<b>APPROXIMATE CONVERSIONS FROM SI UNITS</b>				
Symbol	When You Know	Multiply By	To Find	Symbol
<b>LENGTH</b>				
mm	millimeters	0.039	inches	in
m	meters	3.28	feet	ft
m	meters	1.09	yards	yd
km	kilometers	0.621	miles	mi
<b>AREA</b>				
mm <sup>2</sup>	square millimeters	0.0016	square inches	in <sup>2</sup>
m <sup>2</sup>	square meters	10.764	square feet	ft <sup>2</sup>
m <sup>2</sup>	square meters	1.195	square yards	yd <sup>2</sup>
ha	hectares	2.47	acres	ac
km <sup>2</sup>	square kilometers	0.386	square miles	mi <sup>2</sup>
<b>VOLUME</b>				
mL	milliliters	0.034	fluid ounces	fl oz
L	liters	0.264	gallons	gal
m <sup>3</sup>	cubic meters	35.314	cubic feet	ft <sup>3</sup>
m <sup>3</sup>	cubic meters	1.307	cubic yards	yd <sup>3</sup>
<b>MASS</b>				
g	grams	0.035	ounces	oz
kg	kilograms	2.202	pounds	lb
Mg (or "t")	megagrams (or "metric ton")	1.103	short tons (2000 lb)	T
<b>TEMPERATURE (exact degrees)</b>				
°C	Celsius	1.8C+32	Fahrenheit	°F
<b>ILLUMINATION</b>				
lx	lux	0.0929	foot-candles	fc
cd/m <sup>2</sup>	candela/m <sup>2</sup>	0.2919	foot-Lamberts	fl
<b>FORCE and PRESSURE or STRESS</b>				
N	newtons	0.225	poundforce	lbf
kPa	kilopascals	0.145	poundforce per square inch	lbf/in <sup>2</sup>

# TABLE OF CONTENTS

TECHNICAL DOCUMENTATION PAGE .....	ii
LIST OF FIGURES .....	vi
LIST OF TABLES .....	viii
ACRONYMS, ABBREVIATIONS, AND SYMBOLS .....	ix
EXECUTIVE SUMMARY .....	x
1. INTRODUCTION .....	1
2. OBJECTIVES .....	3
3. LITERATURE REVIEW .....	4
3.1. Elastic Recovery Test and Phase Angle .....	4
3.2. Multiple Stress Creep Recovery (MSCR) .....	4
3.3. Elastic Recovery Test using DSR (ER-DSR) .....	4
3.4. Binder Yield Energy Test (BYET) .....	5
3.5. Linear Amplitude Sweep (LAS) .....	5
3.6. SARA Analysis .....	5
3.7. FTIR Analysis .....	6
4. METHODOLOGY .....	9
4.1. Materials .....	9
4.2. RTFO Aging .....	9
4.3. PAV Aging .....	10
4.4 Rotational Viscosity (RV) Test.....	11
4.5. Dynamic Shear Rheometer (DSR) Test.....	12
4.6. Elastic Recovery test using DSR (ER-DSR) .....	12
4.7. Binder Yield Energy Test (BYET) .....	13
4.8. Multiple Stress Creep Recovery (MSCR) Tests .....	14
4.9. Linear Amplitude Sweep (LAS) Test .....	15
4.10. pH Measurement.....	16
4.11. SARA Analysis.....	17
4.12. NMR Analysis .....	19

4.13. FTIR Analysis.....	19
5. ANALYSIS AND FINDINGS .....	22
5.1. Rotational Viscosity.....	22
5.2. Dynamic Shear Rheometer (DSR).....	22
5.3. Multiple Stress Creep Recovery (MSCR) .....	22
5.4. Elastic Recovery test using DSR (ER-DSR) .....	25
5.5. Binder Yield Energy Test (BYET) .....	27
5.6. Linear Amplitude Sweep (LAS) .....	28
5.7. Correlation between MSCR Percent Recovery (%R) Parameter and Elastic Recovery....	28
5.8. Correlation between MSCR non-recoverable creep compliance ( $J_{nr}$ ) Parameter and Elastic Recovery .....	29
5.9. Correlation between ER-DSR and ER.....	30
5.10. Correlation between the Binder Yield Energy Test (BYET) and Elastic Recovery.....	31
5.11. Relationship of ER-DSR with MSCR, and LAS Test Results .....	34
5.12. pH Measurement.....	35
5.13. SARA Analysis.....	36
5.14. NMR Analysis .....	38
5.15. FTIR Analysis.....	40
6. CONCLUSIONS.....	45
REFERENCES .....	47
APPENDIX A: CHEMICAL TEST RESULTS .....	50
APPENDIX B: MECHANICAL TEST RESULTS .....	52
APPENDIX C: FTIR TEST RESULTS .....	55
C.1. FTIR Spectra for Asphalt Binder Sample .....	55

## LIST OF FIGURES

Figure 1. Rolling thin film oven. ....	10
Figure 2. Pressure aging vessel (PAV). ....	11
Figure 3. Rotational viscometer. ....	11
Figure 4. Dynamic shear rheometer. ....	12
Figure 5. Typical strain curve for elastic recovery test in the DSR (28). ....	13
Figure 6. Typical stress-strain curve and parameter calculation for BYET test (4). ....	14
Figure 7. Determination of the percent recovery and Jnr value. ....	15
Figure 8. Loading scheme for amplitude sweep test damage (AASHTO TP 101-12). ....	16
Figure 9. Separatory funnel. ....	17
Figure 10. pH meter. ....	17
Figure 11. Dissolving asphalt on n-heptane. ....	18
Figure 12. Separation of asphaltene. ....	18
Figure 13. Separation of aromatics, resins, and asphaltenes. ....	19
Figure 14. Evaporation of solvent with a rotary evaporator. ....	19
Figure 15. Real crystal IR (KBr) cards. ....	20
Figure 16. $G^*/\sin\delta$ vs temperature ( $^{\circ}\text{C}$ ) curve for unaged S1 and S2 asphalt binders. ....	22
Figure 17. Percent recovery vs stress for source S1 and S2 asphalt binders. ....	23
Figure 18. Non-recoverable creep compliance vs stress for source S1 and S2 asphalt binders. ..	23
Figure 19. Percent recovery vs stress for additional modified asphalt binders. ....	24
Figure 20. Non-recoverable creep compliance vs stress for additional modified asphalt binders. .....	24
Figure 21. ER-DSR value for the ARDOT-certified unaged asphalt binders (source 1 and 2). ...	25
Figure 22. ER-DSR value for the ARDOT-certified RTFO-aged asphalt binders (source 1 and 2). .....	25
Figure 23. ER-DSR value for the additional unaged modified asphalt binders (source 3 to 10). 26	
Figure 24. ER-DSR value for the additional RTFO-aged modified asphalt binders (source 3 to 8). .....	26
Figure 25. BYET value for the ARDOT-certified RTFO-aged asphalt binders (source 1 and 2). 27	
Figure 26. BYET value for the additional RTFO-aged modified asphalt binders (source 3 to 8). 27	

Figure 27. Number of cycles to failure at 2.5% strain for the ARDOT-certified PAV-aged asphalt binders (source 1 & 2).....	28
Figure 28. Number of cycles to failure at 5.0% strain for the ARDOT-certified PAV-aged asphalt binders (source 1 & 2).....	28
Figure 29. Correlation between MSCR percent recovery (%R) at 3.2 kPa and elastic recovery (AASHTO T 301). ....	29
Figure 30. Correlation between MSCR non-recoverable creep compliance (J <sub>nr</sub> ) at 3.2 kPa and elastic recovery (AASHTO T 301). ....	30
Figure 31. Correlation between ER-DSR (%) for unaged binder and elastic recovery (AASHTO T 301).....	31
Figure 32. Correlation between ER-DSR (%) for RTFO-aged binder and elastic recovery (AASHTO T 301). ....	31
Figure 33. Correlation between the Binder Yield Energy Test (BYET) and elastic recovery (AASHTO T 301). ....	32
Figure 34. Correlation between the strain at peak stress from BYET and elastic recovery (AASHTO T 301). ....	32
Figure 35. Correlation between MSCR percent recovery (%R) at 3.2 kPa and ER-DSR. ....	34
Figure 36. Correlation between number of cycles (N <sub>f</sub> ) at 2.5% strain and ER-DSR. ....	34
Figure 37. Correlation between number of cycles (N <sub>f</sub> ) at 5.0% strain and ER-DSR. ....	35
Figure 38. pH test results. ....	35
Figure 39. SARA fractions for unaged binder samples. ....	36
Figure 40. SARA fractions for RTFO-aged binder samples.....	37
Figure 41. SARA fractions for PAV-aged binder samples.....	37
Figure 42. Gaestel Index (I <sub>c</sub> ).....	38
Figure 43. Typical NMR spectra for the aromatic compounds. ....	39
Figure 44. Typical NMR spectra for the resins compounds. ....	40
Figure 45. Ratio of bonding for source 1 (unaged) binders.....	41
Figure 46. Ratio of bonding for source 2 (unaged) binders.....	41
Figure 47. Ratio of bonding for source 1 (RTFO-aged) binders. ....	42
Figure 48. Ratio of bonding for source 2 (RTFO-aged) binders. ....	42
Figure 49. Ratio of bonding for source 1 (PAV-aged) binders.....	43
Figure 50. Ratio of bonding for source 2 (PAV-aged) binders.....	43



## LIST OF TABLES

Table 1. Nomenclature of binders used from Source 1 and Source 2.....	9
Table 2. Nomenclature of binders from other sources.....	9
Table 3. Superpave specifications for DSR test.....	12
Table 4. Rotational viscosity (mPa.s) test results of binder samples.....	22
Table 5. Summary and ranking of test parameters to replace elastic recovery (AASHTO T 301). .....	33
Table 6. Recommended value of testing parameter against the value of elastic recovery using ductility bath (AASHTO T 301).....	33

## ACRONYMS, ABBREVIATIONS, AND SYMBOLS

AASHTO	American Association of State Highway and Transportation Officials
ALF	Accelerated Loading Facility
ARDOT	Arkansas Department of Transportation
ASTM	American Society for Testing and Materials
BYET	Binder Yield Energy Test
DSR	Dynamic Shear Rheometer
ER	Elastic Recovery
FD	Force Ductility
FHWA	Federal Highway Administration
FTIR	Fourier-Transform Infrared Spectroscopy
G*	Complex Shear Modulus
LAS	Linear Amplitude Sweep
LADOTD	Louisiana Department of Transportation and Development
PAV	Pressure Aging Vessel
PPA	Polyphosphoric Acid
PG	Performance Grade
PMB	Polymer Modified Binders
RTFO	Rolling Thin Film Oven
RV	Rotational Viscosity
SARA	Saturate, Aromatic, Resin and Asphaltene
SBR	Styrene-Butadiene-Rubber
SBS	Styrene-Butadiene-Styrene

## EXECUTIVE SUMMARY

For characterizing the high-temperature performance of modified asphalt binders, many transportation agencies use AASHTO (American Association of Highway and Transportation Officials) T 315 (Standard Method of Test for Determining the Rheological Properties of Asphalt Binder Using a Dynamic Shear Rheometer), which is unable to capture the effects of polymers or acids. Different states Departments of Transportation use the Elastic Recovery (ER) test, a PG Plus method, to evaluate the high-temperature performance of high PG asphalt binders. However, the ER method (AASHTO T 301) is an empirical, expansive and time-consuming. The main objective of the study was to determine the alternative test method(s) to evaluate modified binders as a replacement of the conventional ER test. To this end, three ARDOT-certified PG asphalt binders (PG 64-22, PG 70-22, and PG 76-22) were selected for laboratory testing. In particular, unmodified PG 64-22, PPA-modified PG 70-22, SBS-modified PG 70-22, and SBS+PPA modified PG 76-22 from two different sources were collected. Besides, additional modified asphalt binders (PG 70-22 and PG 76-22) from different sources were also collected for laboratory testing to establish a strong correlation among the test results and make meaningful conclusions.

The Dynamic Shear Rheometer (DSR) based tests including Elastic Recovery using Dynamic Shear Rheometer (ER-DSR), the Multiple Stress Creep and Recovery (MSCR), Linear Amplitude Sweep (LAS), and Binder Yield Energy Test (BYET) were explored. The ER-DSR test was conducted for unaged and RTFO-aged asphalt binders. Two important parameters, percent recovery (%R) and non-recoverable creep compliance (Jnr) from the MSCR test were determined. The binder yield energy (BYE) and strain at peak stress from the BYET were determined at 25°C. The LAS test was conducted using PAV-aged binders to determine the numbers of the cycles at 2.5% and 5.0% strain. Experimental results were used to correlate with ER value. From the correlations, it can be believed that the ER test using ductility bath can be replaced by the ER-DSR test. A very good correlation was found between these two parameters. ER-DSR values of 40%, 50%, and 60% were the representative of 70%, 80%, and 90% ER values using ductility bath. The ER-DSR test can be a good indicator of the presence of elastomer, rutting resistance and binders' toughness and ductility. The MSCR test method can also be considered as an alternative to the ER test method. However, the presence of PPA cannot be determined by either ER-DSR or MSCR test. Therefore, some chemical tests were used in this study to identify the presence of PPA.

The pH measurement test of the binder samples was found to be as a potential tool to compare the stiffness of asphalt binder samples. Though it was to know about asphalt chemistry from pH measurement tests, this test is helpful to trace the presence of acid and degree of modification. The SARA analysis results showed the change in the chemical compositions of asphalt binder due to aging. As mechanistic properties like viscosity and rutting parameters highly depend on the chemical fractions of an asphalt binder sample, this test can be used as an effective tool to predict rutting. Finally, Fourier infrared transformation (FTIR) spectroscopy test was also conducted for selected binders. Comparing these results, it was found that the FTIR test can be used to compare the effect of aging within the binder structure and variation of certain properties (e.g. viscosity and rutting parameter) of asphalt binders.

# 1. INTRODUCTION

The popularity of the use of modified asphalt binders has increased day by day. As a result, additives such as polymers, rubbers, acids, and oils have been used for asphalt modification. Performance properties of asphalt binders such as resistance against high-temperature rutting have been significantly increased due to the modification of the asphalt binder. However, these characteristics cannot be systematically identified by the current Superpave test methods. Different state and local asphalt and highway agencies use different PG plus (PG+) test techniques to capture the presence of polymers, but there is no uniform parameter to characterize the high-grade asphalt binder. Besides, the specification parameters and acceptable limits a largely vary among agencies, and they are adopted and practiced by engineering judgments instead of the asphalt binders' mechanical performance.

Like other state Departments of Transportation (DOTs), Arkansas Department of Transportation (ARDOT) evaluates modified asphalt binders by using a Dynamic Shear Rheometer (DSR) per AASHTO (American Association of State Highway and Transportation Officials) T 315. The AASHTO T 315 method is followed for characterizing modified asphalt binders, but it is unable to capture the effects of elastomeric modification. The Elastic Recovery (ER) test method (AAHSTO T 301) is one of the most commonly used PG Plus test methods to measure the presence of elastomeric modifiers. The AASHTO T 301 test method is useful in confirming that a material has been added to the asphalt to provide a significant elastomeric characteristic, but it does not necessarily identify the type or amount of elastomer added in the modification process.

The 2014 Arkansas Standard Specification for Highway Construction manual states, "PG 70-22 and PG 76-22 asphalt binders shall meet a minimum elongation recovery of 40% and 50%, respectively when tested on the original binder at 25<sup>0</sup>C, in accordance with AASHTO T 301." Other states follow different elastic recoveries and aging conditions. For instance, the Oklahoma DOT requires the ER values of RTFO-aged PG 70-22 and PG 76-28 binders to be at least 65% and 75%, respectively. The Louisiana Department of Transportation and Development (LA DOTD) uses Force Ductility (FD) data in addition to the ER to identify the presence of polymers and quantify its beneficial effects. Recently, both Oklahoma and Louisiana along with some other neighboring states have fully or partially adopted an alternative test method (i.e., MSCR) to characterize polymer modified binders. The ARDOT is still in need of having laboratory performance data to have the confidence to adopt an alternative test method.

Besides MSCR, some other DSR-based asphalt binder tests such as ER-DSR, Linear Amplitude Sweep (LAS), and Binder Yield Energy Test (BYET) have been suggested by other professionals. These test procedures are based on pavement distress mechanisms. The MSCR test method (AASHTO T 350) is meant to replace AASHTO T 315 along with other PG Plus tests. The MSCR parameters i.e. percent recovery (%R) and non-recoverable creep compliance (J<sub>nr</sub>) have been reported to have better relationships with the permanent deformation. The ER-DSR and the BYET have also become popular to replace the current ER, FD and toughness, and tenacity (T&T) test methods. On the other hand, the LAS test has been used as an indicator of asphalt binders' fatigue performance.

However, the mechanical tests (e.g., DSR-based MSCR, ER-DSR, or BYET) may not be appropriate to evaluate high-grade binder modified with chemicals such as polyphosphoric acid (PPA). On the other hand, chemical tests such as SARA (saturates, aromatics, resins, and asphaltenes) analysis or FTIR (Fourier-Transform Infrared Spectroscopy) may provide some

insights about PPA-modified binders. The FTIR has been reported as the first logical step in identifying a polymer into the modified asphalt binder. The FTIR test is also used for quality control of materials and for contamination analysis. However, the FTIR peak(s) to identify PPA and some other chemicals in the binder have not been identified yet. Thus, additional research is needed to find the appropriate test method(s) to characterize both polymer and chemical modified binders, and the current study aims at reducing this research gap.

## **2. OBJECTIVES**

The main objective of the proposed study is to suggest alternative test method(s) to evaluate modified binders as replacements of PG Plus tests. Specific objectives of the current study are:

- i. Evaluate selected ARDOT certified high-grade asphalt binders with respect to local service conditions (temperature and traffic levels) by following the possible alternative test methods including the MSCR, ER-DSR, BYET, and LAS
- ii. Perform chemical analyses (FTIR and SARA) and other mechanistic tests to characterize non-polymeric high PG binders
- iii. Propose simple and effective test methods for characterizing non-polymeric high PG grade binders
- iv. Develop guidelines toward adopting the appropriate test method(s) so that neither suppliers nor users are penalized

### 3. LITERATURE REVIEW

The usage of polymer modified asphalt binders has increased extensively in pavement engineering due to requirements of high resistance against rutting, thermal cracking, fatigue cracking, stripping, and temperature susceptibility (1-2). But, the existing Performance Grade (PG) test methods are not suitable to determine the mechanical properties of the polymer-modified binders beyond the linear viscoelastic range. This is because the conventional Superpave tests were developed only to characterize the unmodified asphalt binders (3).

#### 3.1. Elastic Recovery Test and Phase Angle

Elastic recovery (ER) test using the ductility bath and the parameter phase angle both are being used by some state DOTs. The ER test and phase angle parameter used as an indicator to identify the elastomeric modifiers. The elasticity of the asphalt binder is correlated with the rutting and fatigue cracking resistance. The elasticity of the asphalt binder is increased due to the decrease of the phase angle (4). D'Angelo and Mehta et al. stated that the phase angle has a correlation with elastomeric modification type but does not have any absolute correlations with field performance (5-6). Mehta et al. tested different types of modified binders and concluded that the ER test (AASHTO T 301) is not effective compared to the other PG Plus tests (6). Clopotel et al. (7) also studied modified asphalt binders and tried to develop a correlation between the elastic recovery test and asphalt binders' fatigue. But the research team did not find any correlation between the elastic recovery test and the fatigue life. On the other hand, an old test named Toughness and Tenacity (T&T) is being used to measure the elastomeric properties of asphalt binder (8).

#### 3.2. Multiple Stress Creep Recovery (MSCR)

For characterizing PG asphalt binders, many state agencies follow AASHTO M320 "Standard Specification for Performance-Graded Asphalt Binder." However, the applicability of AASHTO M320 specification for polymer-modified asphalt binders has been questioned by many industries and state highway agencies. AASHTO M 332 "Performance-Graded Asphalt Binder Using the Multiple-Stress Creep-Recovery (MSCR) Test" has been suggested as a substitution of AASHTO M320. It is proposed for a better understanding of the polymer effect inside the modified binder (9). The MSCR parameters i.e. percent recovery (%R) and non-recoverable creep compliance ( $J_{nr}$ ) have a better relationship with the permanent deformation (10). The Federal Highway Administration (FHWA) sponsored a project that studied the accelerated loading facility (ALF) and observed a linear correlation between  $J_{nr}$  and rutting with an  $R^2$  value of 0.82 (11). In AASHTO M 332, the  $J_{nr}$  is now stated as an alternative for the grade bumping system. Recently, some state agencies have specified that the high-temperature PG grade should be bumped to account for slow traffic and high traffic volumes based on binder's  $J_{nr}$  (12).

#### 3.3. Elastic Recovery Test using DSR (ER-DSR)

The elastic recovery test using a DSR (ER-DSR) has been proposed as an alternative to the current elastic recovery test using a ductility bath and Toughness and Tenacity (T&T) test method. A few laboratory studies have been done to correlate the elastic recovery (AASHTO T 301) with the elastic recovery using DSR. For instance, Clopotel et al. (7) used two different base binders and five different modifications in their study. They found a linear correlation between the two elastic recovery procedures with an  $R^2$  value of 0.97. However, poor

correlations existed between the ER-DSR test and binder's fatigue performance. Currently, the ER-DSR is being considered as a provisional standard by the AASHTO.

### **3.4. Binder Yield Energy Test (BYET)**

Binder Yield Energy Test (BYET) has been also planned as alternatives to the current elastic recovery test using a ductility bath and the T&T test method. Tabatabaee et al. (13) derived a linear relationship between BYET strain at peak stress and binder ductility of selected modified asphalt binders (13). However, no relationship was between the elastomerically modified binders and unmodified binders were reported. Besides, no literature has been found that correlates binder yield energy and toughness and tenacity (4). As a result, AASHTO TP 123 "Measuring asphalt binder yield energy and elastic recovery using the dynamic shear rheometer" has been considered as a provisional standard by the AASHTO (14). It is claimed that AASHTO TP 123 can promisingly predict low-temperature fatigue and thermal cracking properties of asphalt binders (15).

### **3.5. Linear Amplitude Sweep (LAS)**

Linear Amplitude Sweep (LAS) test was developed at the University of Wisconsin-Madison by Johnson et al. and modified by Hintz et al. to indicate asphalt binder fatigue (16-17). At first, a frequency sweep test is conducted to measure the asphalt binder's linear viscoelastic properties. Then, a strain amplitude sweep is conducted from 1% strain to 30% strain at a constant frequency of 10Hz. After the end of the test, viscoelastic continuum damage mechanics are used to analyze the test data (17).

### **3.6. SARA Analysis**

Asphalt binder is a complex organic material consisting of a large number of hydrocarbons and can be divided into four fractions: Saturates, Aromatics, Resins, and Asphaltenes; commonly known as SARA fractions. Many researchers focused on studying the impact of aging on the chemical composition of asphalt binders. Wang et al. (18) studied the effect of aging on SBS-modified asphalt on the performance on asphalt pavement. As usual, the short-term aging of this study was performed on SBS-modified asphalt binders by using a Rolling Thin Film Oven (RTFO). Several tests were conducted to observe the mechanistic properties (penetration, softening point, ductility, viscosity, toughness etc.) of these short-term aged samples. From the test results, it was observed that the penetration and ductility of the modified samples decreased after SBS modification, but the softening properties had increased. The researchers were also able to validate an aging dynamic model with viscosity. It was also observed that the modifier (SBS) particle area was well correlated with the change of aging temperature.

Sultana and Bhasin (19) investigated the impact of chemical compositions on the rheological and mechanical properties of asphalt binders. These researchers focused on investigating the relative concentration of different polar fractions on the rheology and tensile strength of asphalt binders. In this study, PG 64-16 and PG 67-22 binders, and four other derivative binders were doped with each of the four fractions (Saturates, Aromatics, Resins, and Asphaltenes). Binders with higher polar fractions exhibited higher stiffness and tensile strength. Moreover, binders with higher percentages of Resins and Asphaltenes showed both higher stiffness and higher tensile strength.

Weigel and Stephen (20) focused on finding the interrelationship between the chemical fractions of asphalt binder and its materials characteristics. They studied 11 binder samples of different



levels of aging with four different types of aggregates. The SARA fractions showed a strong influence on mechanistic properties (stiffness, viscosity, deformation behavior, and temperature sensitivity) of asphalt binders. These researchers also claimed that Asphaltenes play a major role in the aging behavior. It was observed that binder-aggregate interaction depends mostly on the adhesion properties. Some other factors such as Silicon Dioxide content and surface charge affect the adhesion properties. Their research observed a significant influence of the SARA fractions on the physical, rheological, aging and adhesion behavior of the properties of asphalt binders.

Alam and Hossain (21) studied asphalt binder modified with PPA and SBS. In this study, the base binders were collected from two different crudes: Canadian Crude and Arabian Crude. From several test results, it was found that the addition of PPA increased the Asphaltene contents as well as increased the viscosity of asphalt binder. They also observed that SBS modification rearranged the SARA fractions rather than changing the percentages. A different group of researchers claimed that SBS performed far better than the combination of PPA and SBS or PPA alone. Paliukaite et al. (22) described a well-established model for the colloidal stability of asphalt binders. Among the chemical fractions of asphalt binder, Asphaltenes are highly polar and dispersed in a system of Aromatics and Resins. The solubility of Asphaltene determines the colloidal stability of an asphalt binder which can be determined by Gaestel Index (Ic). The Gaestel index can be determined by using Equation 1.

$$\text{Gaestel Index (Ic)} = \frac{\% \text{ Saturates} + \% \text{ Asphaltenes}}{\% \text{ Aromatics} + \% \text{ Resins}} \quad [1]$$

A higher Gaestel Index indicates an unstable colloidal structure, whereas a lower Gaestel Index means the binder is soft and colloiddally unstable. In a practical context, neither too high nor too low Gaestel Index is desirable.

### 3.7. FTIR Analysis

The FTIR spectroscopy technique can be applied on asphalt binder samples to detect specific functional groups and any change in the amount of the functional group due to modification of asphalt. In this technique, IR signatures of certain structural characteristics of any chemical group or molecule can be interpreted from their FTIR spectra (23).

Lamontagne et al. (24) used the FTIR spectroscopy technique to evaluate the asphalt oxidation process due to short-term and long-term aging. They found that the sulphoxide function rate increased significantly in all initial periods (first two years) and stabilizes thereafter. The bitumen with high sulphoxide rate at the start was the most sensitive to the oxidation. The Aromatic rate followed the same approach as carbonyl formation, during the first two years. The resulting effect was the increase of the relative rate of the adjacent aromatic hydrogens within structure periphery. Moreover, researchers of this project drew a distinct difference between road aging and thermal oxidations. It was further reported that RTFO-aging itself does not induce any significant chemical aging, but the PAV-aging generates important chemical changes. This is why; the laboratory aging process is less stabilized than the field demonstration process.

Nasrekani et al. (25) performed the FTIR spectroscopy using an appropriate spectrometer to observe the impact of blending gilsonite with asphalt binder. They tested both bituminous sample

and gilsonite powder disk, which they used as a modifier in the range of 4000 to 400  $\text{cm}^{-1}$  with 32 scans per analysis at a resolution of 4  $\text{cm}^{-1}$ . Furthermore, a quantitative comparison was performed using spectrometric indices. These specific structural and functional indices were calculated using the valley to valley integration between peak points. Based on the literature review done this specific group of researchers, carbonyl and sulfoxide indices were determined using Equations 2 and 3.

$$\text{Carbonyl Index} = A_{1700} / \Sigma A \quad [2]$$

$$\text{Sulfoxide Index} = A_{1030} / \Sigma A \quad [3]$$

where,  $\Sigma A = A_{1700} + A_{1600} + A_{1460} + A_{1376} + A_{1030} + A_{864} + A_{814} + A_{743} + A_{724} + A_{(2953+2923+2862)}$ . In these equations,  $A_x$  is the area under the peak at  $x$  ( $\text{cm}^{-1}$ ) wavenumber.

The FTIR spectroscopy and functional group indices of bitumen also help to anticipate the moisture sensitivity of bitumen-aggregate. The similarity throughout the spectra was noticeable in 2920, 2850, 1600, 1455, 1375 and 1030  $\text{cm}^{-1}$  wavenumber (8). Both samples used in their study show peaks at these wavenumbers. Absorbance at 2920 and 2850  $\text{cm}^{-1}$  were found related to asymmetric and symmetric C-H stretching vibrations, respectively. The peak intensity at 2920  $\text{cm}^{-1}$  indicated the presence of long aliphatic chains in both Gilsonite and refined bitumen. Significant similarities between functional groups of Gilsonite powder modified binders and neat binders were observed (especially at wavenumbers above 1400  $\text{cm}^{-1}$ ). This result confirmed Gilsonite as a natural bitumen-based material. It was also observed that both carbonyl and sulfoxide indices are decreased by blending gilsonite with neat bitumen. A high-intensity peak was also observed for Gilsonite powder at 1030  $\text{cm}^{-1}$ , the decrease in sulfoxide index was not expected. Moreover, it was concluded that other aliphatic functional groups and Asphaltenes resulted in an overall reduction of the sulfoxide ratio in the bitumen, whereas an increase in sulfoxide groups and carboxylic acids of bitumen would result in lower moisture resistance of asphalt concrete.

Fini et al. conducted FTIR tests to observe the reformation of organic matter in swine manure into the oil with heat and pressure in anoxic and aqueous conditions (26). The product oil contains a significant amount of Asphaltene and Resins. In order to produce bio-binder usable for crack sealant in pavements, materials needed to be engineered with specific rheological properties required using in the pavement. For ensuring desirable longer performance; physical, chemical and rheological properties of the bio-binder, the effects of aging and the stability of the material must be quantified. These researchers also compared their test results with corresponding petroleum-asphalt binders and observed a lower concentration of Saturates and a very low (almost zero) naphthene The Aromatic contents in a bio-based binder is higher than that in a petroleum-based binder. Moreover, the interaction of some of the polar functional groups was found, which enable the bio-binder to exhibit higher moisture resistance and the high polar contents of this bio-binder increase its potentiality as a crack and joint sealant. From the FTIR test results, a significant difference was found between the common peaks and regions assigned to C-H and C-C bond especially in the regions 600–900  $\text{cm}^{-1}$  and 2700–3000  $\text{cm}^{-1}$ . But the common region selected for evaluation of the extent of aging extent was at 1700  $\text{cm}^{-1}$  for carbonyl and 1000  $\text{cm}^{-1}$  for sulfoxide were not distinguishable from the large mixture of peaks

throughout these regions. A large shoulder was detected next to the twin towers from 3000–3300  $\text{cm}^{-1}$  which basically emerged due to the presence of a mixture of amines, aromatics, alcohols, and olefins. Thus, FTIR spectra were used evaluated qualitatively only form certain known information of the material.

Yao et al. (27) aimed to improve the rutting and fatigue cracking resistance of asphalt using nano or macro size materials as modifiers and examine the microscopic change induced by such modification. Modifiers were added to control binder using high shear mix and FTIR tests were carried out to investigate the microstructure performance of asphalt binders. The complex mixtures of organic molecules from the binders go through partial oxidation reactions which causes a structural modification in chemical compositions and changes in the component distributions. Due to oxidation, the bonding between chemical elements is altered and the interaction between the modules is changed. These variations were tracked through the FTIR spectroscopy. These researchers found significant changes in chemical bond before and after the RTFO- and PAV-aging. The degree of oxidation indicated by the carbonyl index decreased slightly after the RTFO aging process, but it increased significantly after the PAV aging. The sulfoxide index ratio also decreased after the RTFO- and PAV-aging processes. Researchers also found a significant impact of aging on chemical fractions from FTIR tests. During the aging process of asphalt binder, the Resins and Asphaltenes contents reacted with oxygen and subsequently increased the ratios of the aromatic index. Structurally, Aromatic is a hydrocarbon with planar structure and can be characterized by double or single bonds between stacked carbon rings. On the other hand, aliphatic is a non-planar structure with single carbon bonds, therefore, structures do not stack over. The differences in the chemical structures contribute to the variation of the properties of aromatic and aliphatic contents. After aging, the aromatic index ratio increased, and aliphatic index ratio decreased in the modified asphalt binder relative to the control asphalt binder. The maltene factions dissolved in aliphatic hydrocarbons reacted with the oxygen to form Asphaltenes which subsequently hydrogenated into the Aromatics. The control asphalt showed a different line trend of FTIR than modified asphalt binder. Researchers identified the possibility of reactions between modifiers and asphalt as the reason for the difference in the trend which can be further investigated from the FTIR test results.

## 4. METHODOLOGY

### 4.1. Materials

Three ARDOT-certified asphalt binders (PG 64-22, PG 70-22 and PG 76-22) were selected for laboratory testing. In particular, unmodified PG 64-22, PPA-modified PG 70-22, SBS-modified PG 70-22, and SBS+PPA modified PG 76-22 from two different sources have been collected. The nomenclature was developed for the study to identify the samples and shown in Table 1.

Table 1. Nomenclature of binders used from Source 1 and Source 2.

Binders	Modifiers	Canadian Crude Source (S1)	Arabian Crude Source (S2)
PG 64-22	N/A	S1B1	S2B1
PG 70-22	PPA	S1B2	S2B2
PG 70-22	SBS	S1B3	S2B3
PG 76-22	SBS+PPA	S1B4	S2B4

Besides, additional 16 modified binders (PG 70-22 and PG 76-22) from eight (8) different sources were used for laboratory testing to develop meaningful comparisons and contrast among the test results. The nomenclature for the additional binders is shown in Table 2.

Table 2. Nomenclature of binders from other sources.

Source Name	Performance Grade	Binder ID
Source 3	PG 70-22	S3B3
Source 3	PG 76-22	S3B4
Source 4	PG 70-22	S4B3
Source 4	PG 76-22	S4B4
Source 5	PG 70-22	S5B3
Source 5	PG 76-22	S5B4
Source 6	PG 70-22	S6B3
Source 6	PG 76-22	S6B4
Source 7	PG 70-22	S7B3
Source 7	PG 76-22	S7B4
Source 8	PG 70-22	S8B3
Source 8	PG 76-22	S8B4
Source 9	PG 70-22	S9B3
Source 9	PG 76-22	S9B4
Source 10	PG 70-22	S10B3
Source 10	PG 76-22	S10B4

### 4.2. RTFO Aging

The asphalt binder samples are aged to observe the change in mechanistic properties due to aging. For short term aging, a Rolling Thin Film Oven (RTFO) has been used in accordance with AASHTO T 240. Later, the short-term aged samples are used for long term aging and as well as for other mechanistic tests. For the RTFO aging, an asphalt binder is heated to a point when it is fluid enough to pour into the bottles. The heating chamber of RTFO must be preheated up to 163°C. After preheating, the bottles will be filled with samples before placing inside the hot chamber of RTFO (Figure 1) and the door will be locked to prevent heat loss. The sample rack is

set to rotate at 15 rpm and airflow of 4L/min is directly blown in the bottles for 85 minutes. The combination of airflow and heat occur oxidation of asphalt binder as well as subsequent short-term aging.



**Figure 1. Rolling thin film oven.**

### **4.3. PAV Aging**

Pressure Aging Vessel (PAV) aging is used to simulate the long-term aging of asphalt binder samples. As asphalt binders remain exposed to nature throughout entire service life, experience longer oxidation period, which causes long-term aging. Long term aging makes a binder stiffer and susceptible to low temperature cracking. The RTFO-aged samples are taken under long term aging with a PAV as per AASHTO R 28. At first, the temperature is set at 100°C for running the aging process. After reaching the anticipated temperature, the RTFO aged samples are placed in a pan. Later these samples are staked into the specially designed vertical rack and then put inside the PV chamber (Figure 2) for long term aging. An air pressure of 2.10 MPa is supplied from an outside cylinder. After achieving the required combination of temperature and pressure, aging is continued for approximately 20 hours. After the PAV aging, the chamber is depressurized, and the aged samples are taken out of the chamber and stored for further chemical and mechanical testing.



**Figure 2. Pressure aging vessel (PAV).**

#### **4.4 Rotational Viscosity (RV) Test**

The Rotational Viscometer (RV) is done to determine the viscosity of asphalt binders in the high-temperature range (135°C to 180°C) following AASHTO T 316. This test helps to determine the mixing and compaction temperatures of asphalt binders. The RV test considers the torque required to maintain a constant rotational speed of a cylindrical spindle submerged in an asphalt binder at a constant temperature. The equivalent viscosity of this torque is given as the output in the rotational viscometer (Figure 3).



**Figure 3. Rotational viscometer.**

#### 4.5. Dynamic Shear Rheometer (DSR) Test

The Dynamic Shear Rheometer (DSR) (Figure 4) test is conducted on unaged, RTFO-aged, and PAV-aged binders for characterizing their viscoelastic properties. In this test, two specific properties of a sample are tested: Complex Shear Modulus ( $G^*$ ), which represents the total resistance offered by the asphalt binder under repeated shear loading and phase angle ( $\delta$ ), which represents the delay in the resulting shearing strain in an asphalt binder specimen in response to an applied shear stress. The Superpave rutting and fatigue factors depend on these parameters. The DSR test is conducted by following AASHTO T 315. Asphalt binder samples are sandwiched between two parallel plates geometry. Then shearing stress is applied on the binder sample at a loading rate of 10 rad/sec (corresponding to 55 mph vehicle speed). For 25 mm parallel plates, the intermediate gap should be as much as 1.00 mm. For 8.00 mm plates, the gap should be 2.00 mm. The Superpave specifications for the rutting and fatigue factors are given in Table 3.

Table 3. Superpave specifications for DSR test.

Binder Sample	Value	Test Temperature (°C)	Specification
Unaged binder	$G^*/\sin\delta$	High Service	$\geq 1.00$ kPa (0.145 psi)
RTFO-aged binder	$G^*/\sin\delta$	High Service	$\geq 2.20$ kPa (0.319 psi)
PAV-aged binder	$G^*.\sin\delta$	Intermediate Service	$\leq 5000$ kPa (725 psi)

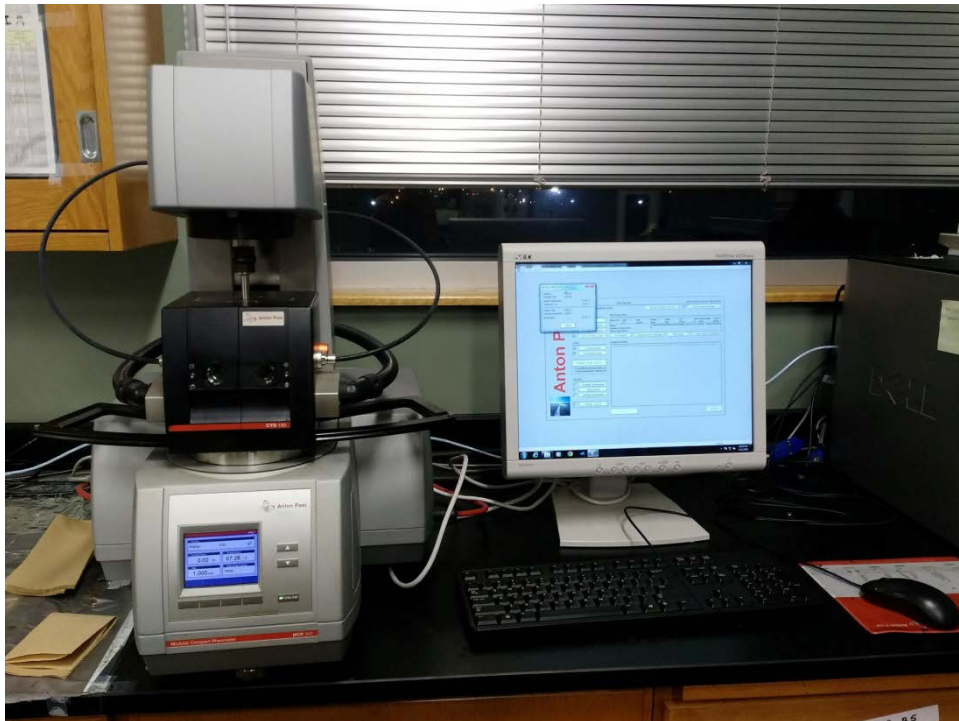


Figure 4. Dynamic shear rheometer.

#### 4.6. Elastic Recovery test using DSR (ER-DSR)

The primary objective of this test is to find the elastic recovery and ductility of the asphalt binder. Although multiple tests are available to determine elastic recovery, the ER-DSR test

method is developed for an advantage of testing in a DSR rather than in an alternative testing apparatus. For conducting the elastic recovery procedure in the DSR, 8 mm samples are prepared and placed in the DSR's parallel plate geometry at a temperature of 25 °C. These 8 mm samples are loaded at a shear rate of 2.30% s<sup>-1</sup> up to a strain level of 278% (AASHTO T 301). Then the load is removed from the sample for a duration of 30 min. A typical stress-strain curve for ER-DSR test is shown in Figure 5. Elastic recovery in the DSR is calculated using Equation 4.

$$\text{Elastic Recovery} = \frac{\gamma_2}{\gamma_1} \times 100\% \quad [4]$$

where:

$\gamma_2$  = Recovered strain at 1800 seconds after removal of load and

$\gamma_1$  = Peak strain.

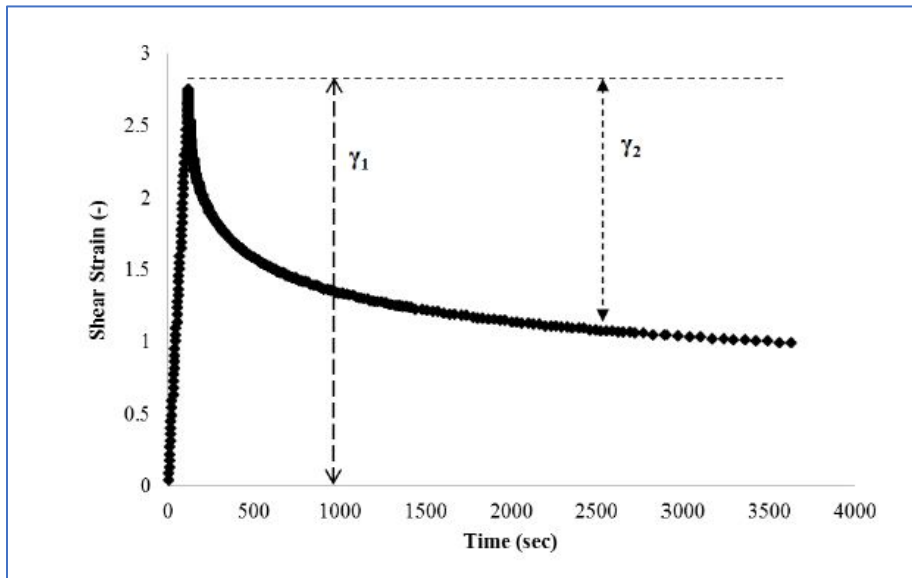


Figure 5. Typical strain curve for elastic recovery test in the DSR (28).

#### 4.7. Binder Yield Energy Test (BYET)

The Binder Yield Energy Test (BYET) is conducted to predict the fatigue performance of the binder. This test setup is done by preparing an 8 mm sample and placing it in the DSR 8 mm geometry. Then a shear load is applied to the sample at a rate of 2.30% s<sup>-1</sup> until a 4140% strain is reached. During the loading of the specimen, stress, and strain are recorded for the entire process. Figure 6 shows a typical shear stress-strain curve for the BYET. The test is performed with a DSR and gives two parameters as output: yield energy and shear strain at maximum shear stress. The yield energy is the area under the curve until the sample yields, which represents the toughness of an asphalt binder and the shear strain at the maximum shear stress at peak stress represents the ductility of an asphalt binder sample.



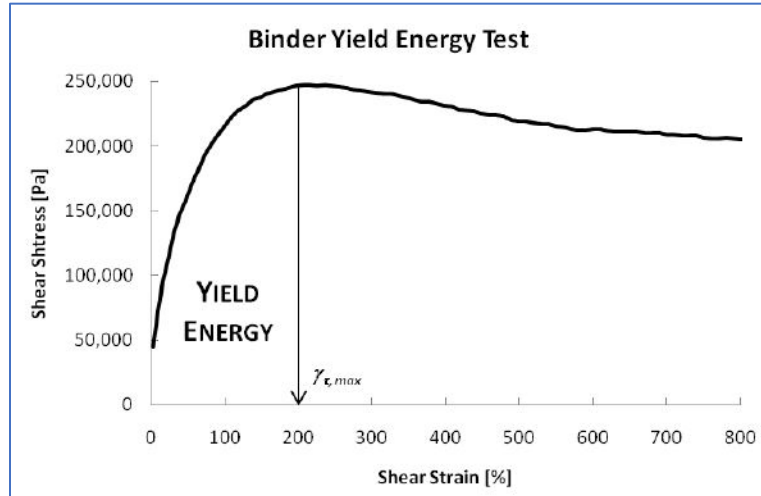


Figure 6. Typical stress-strain curve and parameter calculation for BYET test (4).

#### 4.8. Multiple Stress Creep Recovery (MSCR) Tests

The PG specifications are not always effective to characterize the rutting and fatigue behavior of polymer modified binders. Bahia et al. (29) reported that the Superpave test methods were not suitable enough to characterize the polymer modified binders as the Superpave specifications were considering unmodified binders only. To resolve this limitation, Bahia et al. (30) developed a test method known as the RCRT method. The RCRT method itself has some limitations. One of the major limitations is that this method only considers lower stress levels than the actual traffic loading for measuring the permanent strain of binders. Moreover, at lower stress levels, a majority of polymer modified binders barely shows the nonlinear behavior. To resolve this issue, the Federal Highway Administration (FHWA) modified the RCRT method by increasing stress levels which is currently known as the MSCR test method (31). The MSCR test method (AASHTO T 350) is developed based on the well-established creep and recovery test concept. In the MSCR test method, one-second shearing creep load is applied on the RTFO-aged asphalt binder by using a dynamic shear rheometer. The load is removed after one second. Then, the test sample is allowed to release the creep load for nine seconds. A low-stress level of 0.1 kPa for 10 creep/recovery cycles is applied at first which is then increased to 3.2 kPa. This process has been repeated for an additional 10 cycles. Load application pattern for the MSCR test is shown in Figure 7. There are two major output parameters found from the MSCR test: the compliance ( $J_{nr}$ ) and the percent creep recovery (%R). The  $J_{nr}$  value is the amount of residual strain left in the binder within the linear and nonlinear viscoelastic range for higher temperatures and higher stress levels. On the other hand, the percent creep recovery (%R) measures the extent of asphalt specimen returns to its original position after the load has been removed.

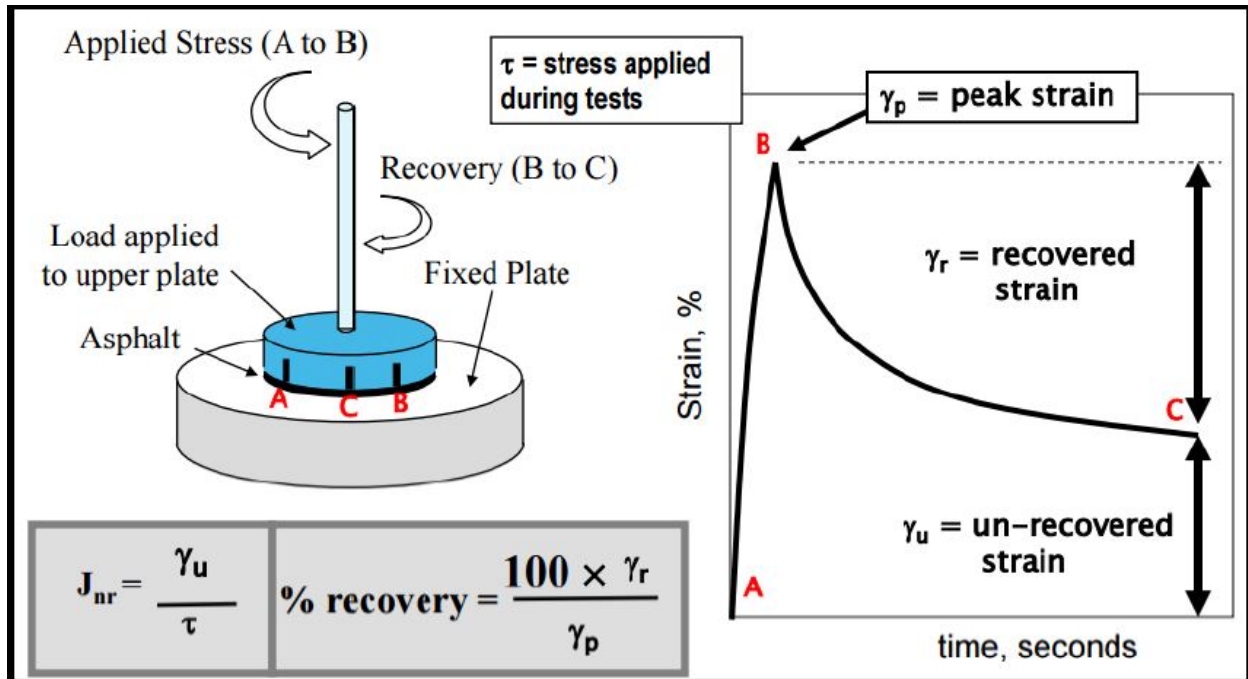


Figure 7. Determination of the percent recovery and Jnr value.

#### 4.9. Linear Amplitude Sweep (LAS) Test

The purpose of the LAS is to evaluate the fatigue damage resisting the ability of asphalt binders. During this test, a cyclic load is usually applied by using a DSR machine that increases the strain amplitudes accelerate damage (AASHTO TP 101-12). A Modular Compact Rheometer MCR 302, Version: Rheoplus32 V3.62 was used for conducting the Linear Amplitude test where samples with 8 mm diameter and 2 mm thickness were used. This test method consists of two steps: a frequency sweep test to determine the undamaged properties and an amplitude sweep to simulate accelerated damage. The frequency sweep test was performed by maintaining binder's intermediate temperature (the temperature at  $G^* \sin \delta = 5,000 \text{ kPa}$ ) to resist the fatigue damage and a constant 0.1% oscillatory shear loading over a range of frequencies from 0.2-30 Hz. Moreover, the rheological properties of the binder were measured by using the frequency sweep test at selected temperatures for developing the master curves. After the frequency sweep test, an amplitude sweep test is started on the same binder sample by using DSR manufacturer's controller software. The amplitude sweep test was conducted at the same temperature but at different loading frequencies and load amplitudes than the frequency sweep test. A constant frequency of 10Hz was used to perform the test. Initially, a 0.1% strain was applied for the first 100 cycles for measuring the undamaged properties of within the linear viscoelastic region of the asphalt binder samples. Each of the succeeding load steps consists of 100 cycles at a rate of increase of 1% applied strain per step for 30 steps, beginning at 1% and ending at 30% applied strain. The graphical example of loading scheme of amplitude sweep test is shown in Figure 8.

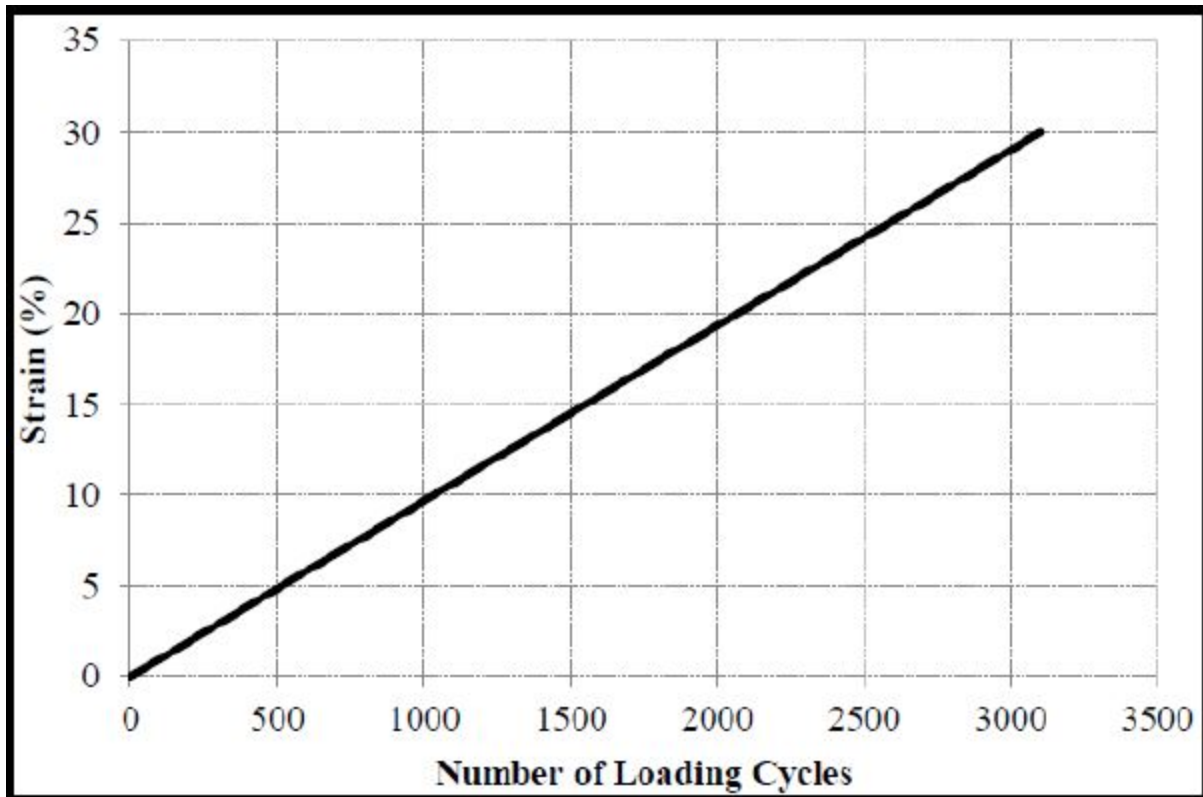
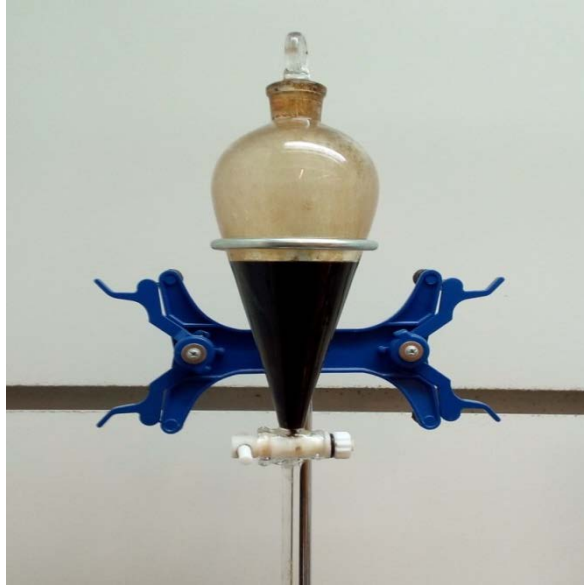


Figure 8. Loading scheme for amplitude sweep test damage (AASHTO TP 101-12).

#### 4.10. pH Measurement

The acidity level of the binder is measured to observe if there is any change in the pH in the binder due to its modification. For measuring the pH of a binder, 5 gm sample binder will be taken in a 250 mL beaker. Then, 30 ml of toluene will be added. The beaker is heated slowly to dissolve the binder. The sample is allowed to cool down to room temperature and transferred to a 250 mL separatory funnel (Figure 9). 15 mL of de-ionized water is added. Then, the separatory funnel should be shaken for 2 minutes to extract the water-soluble materials from toluene into the aqueous layer. Contents of the separatory funnel will be centrifuged to separate the aqueous layer is set aside. The toluene layer is then poured back into the separatory funnel extracted. A pH meter (Figure 10) is used to measure the pH from the extract.



**Figure 9. Separatory funnel.**



**Figure 10. pH meter.**

#### **4.11. SARA Analysis**

All binder samples are characterized based on their chemical composition. The main constituents of any asphalt binders are: Saturates(S), Aromatics (A), Resins (R), and Asphaltenes (A). The SARA fractions of the binders are determined following the standard ASTM D 4124-09. First of all, the binder sample should be dissolved into n-heptane. A stirring magnet was added into the round bottom flask to ensure the proper mixing of the asphalt binder sample into n-heptane solvent (Figure 11). The stirring action continued for 1 to 2 hours until the asphalt binder completely dissolved into n-heptane. A Buchner-style fritted glass funnel of medium porosity

(ASTM 10-15 micrometer) was used for the filtering operation which separated the Asphaltene from the Maltene within the solvent (Figure 12). The maltene fractions contain Saturate, Aromatics and Resins fractions in the solvent which were later separated through column chromatography (Figure 13). The separated solvent fractions were taken to a rotary evaporator for solvent-removal (Figure 14). The eluted fractions were not allowed to dry voluntarily as the solvents do not evaporate entirely through voluntary evaporation. The separated fractions were recorded for their dried masses and expressed as  $M_{Saturates}$ ,  $M_{Aromatics}$ , and  $M_{Resins}$  for the Saturates, Aromatics, and Resins fractions, respectively. The masses were expressed as percent fractions of the original sample that was taken. About 90~99 % of the whole sample could be recovered through this column chromatography technique.



**Figure 11. Dissolving asphalt on n-heptane.**



**Figure 12. Separation of asphaltene.**



Figure 13. Separation of aromatics, resins, and asphaltenes.



Figure 14. Evaporation of solvent with a rotary evaporator.

#### 4.12. NMR Analysis

NMR analysis tests were conducted on separated Aromatics and Resins fractions achieved SARA analysis for evaluating their purity. There are many versions of NMR spectroscopy, whereas Proton nuclear magnetic resonance (proton NMR, hydrogen-1 NMR, or  $^1\text{H}$  NMR) was used to evaluate the separation of Aromatics and Resins.

#### 4.13. FTIR Analysis



The FTIR technique can be applied on an asphalt binder to spectroscopically detect the presence or change in quantities of functional groups that might have occurred due to the modification (2). Characteristics of the functional groups can be associated with FTIR spectra which correspond to the fundamental vibrations of the functional groups (32-33). There are two types of vibration possible in infra-Red: Stretching and bending. Molecules with simple diatomic structure have only one bond, which may stretch. In the case of polyatomic molecules, each atom with three degrees of freedom in three directions is perpendicular to each other. Thus, a molecule of  $n$  atoms has  $3n$  degrees of freedom.

A normal mode of vibration can be considered infrared active if it absorbs the incident infrared light due to a change in the dipole moment of the molecule during the course of the vibration. Thus, symmetric vibrations are usually not detected in infrared as all vibrations are symmetrical with respect to the center of symmetry. In another way, the asymmetric vibrations of all molecules are detected due to lack of selectivity allows probing the properties of almost all chemical groups in one sample.

Chemical groups with permanent dipole (polar) exhibit strong IR absorptions with two main types of vibrations: vibrations along with chemical bonds which involve bond-length changes, called stretching vibrations and vibrations involving changes in bond angles called bending vibrations. The vibration frequency depends on factors like the mass of the atoms, bond strength, with higher frequencies for triple or double bonds as compared to single bonds. With the help of FTIR, it is possible to observe any alteration in vibration frequency within the Infra-Red spectra. The vibrational frequency of a given chemical group is expected in a specific region depending on the type of atoms involved and the type of chemical bonds. Thus, to observe any change between the infrared mode frequency and the structural properties due to modification of asphalt, the IR analysis can be performed using theoretical chemistry approaches.



**Figure 15. Real crystal IR (KBr) cards.**

The FTIR tests for the samples were conducted with a Nicolet 8700 spectrometer. During this test, vibrational Infra-Red (IR) light is passed through disposable Real Crystal IR (KBr) cards (Figure 15) without sample and recorded as background data. Then similar procedures are followed with cards with the sample. Combining these two sets of data, spectra for the samples has been developed. A wavenumber range of 450 cm<sup>-1</sup> to 4500cm<sup>-1</sup> has been considered for analysis. For observing the ratio of bonding, the following wavelength and Equations 5, 6, 7, 8, 9, and 10 have been followed (9).

$$I_{\text{CH=CH}} = \frac{\text{Area of the ethylene band centered around } 966 \text{ cm}^{-1}}{\Sigma \text{Area of the spectral band between } 450 \text{ cm}^{-1} \text{ and } 4500 \text{ cm}^{-1}} \quad [5]$$

$$I_{\text{S=O}} = \frac{\text{Area of the sulfoxide band centered around } 1030 \text{ cm}^{-1}}{\Sigma \text{Area of the spectral band between } 450 \text{ cm}^{-1} \text{ and } 4500 \text{ cm}^{-1}} \quad [6]$$

$$I_{\text{C-H of CH}_3} = \frac{\text{Area of the aliphatic branched band centered around } 1376 \text{ cm}^{-1}}{\Sigma \text{Area of the spectral band between } 450 \text{ cm}^{-1} \text{ and } 4500 \text{ cm}^{-1}} \quad [7]$$

$$I_{\text{C-H of }-(\text{CH}_2)_n-} = \frac{\text{Area of the aliphatic index band centered around } 1460 \text{ cm}^{-1}}{\Sigma \text{Area of the spectral band between } 450 \text{ cm}^{-1} \text{ and } 4500 \text{ cm}^{-1}} \quad [8]$$

$$I_{\text{C=C}} = \frac{\text{Area of the aromatic band centered around } 1600 \text{ cm}^{-1}}{\Sigma \text{Area of the spectral band between } 450 \text{ cm}^{-1} \text{ and } 4500 \text{ cm}^{-1}} \quad [9]$$

$$I_{\text{C=O}} = \frac{\text{Area of the carbonyl band centered around } 1690 \text{ cm}^{-1}}{\Sigma \text{Area of the spectral band between } 450 \text{ cm}^{-1} \text{ and } 4500 \text{ cm}^{-1}} \quad [10]$$



## 5. ANALYSIS AND FINDINGS

### 5.1. Rotational Viscosity

From the rotational viscosity test results, SBS+PPA modified binders S1B4 and S2B4 showed the highest viscosity compared to the other binders. Only PPA modified asphalt binders S1B2 and S2B2 had higher viscosity compared to the neat binders but lower than other modified binders. On the other hand, SBS modified binders S1B3 and S2B3 showed viscosity higher than PPA modified binders but lower than SBS+PPA modified binders. Therefore, the mixing and compaction temperatures are expected to increase for the modified binders. The RV test results are shown in Table 4.

Table 4. Rotational viscosity (mPa.s) test results of binder samples.

Temperature	S1B1	S1B2	S1B3	S1B4	S2B1	S2B2	S2B3	S2B4
135°C	504	733	1,271	1,929	445	645	1,271	1,767
150°C	254	325	595	870	208	295	554	758
165°C	145	162	312	450	112	145	279	350
180°C	75	75	175	262	62	75	162	187

### 5.2. Dynamic Shear Rheometer (DSR)

The dynamic shear modulus test was conducted for unaged binders. The complex shear modulus increased, and phase angle decreased for modified asphalt binders. Therefore, the rutting factor ( $G^*/\sin\delta$ ) increased for modified binders, as shown in Figure 16. The failing temperature with respect to rutting also increased for modified asphalt binders.

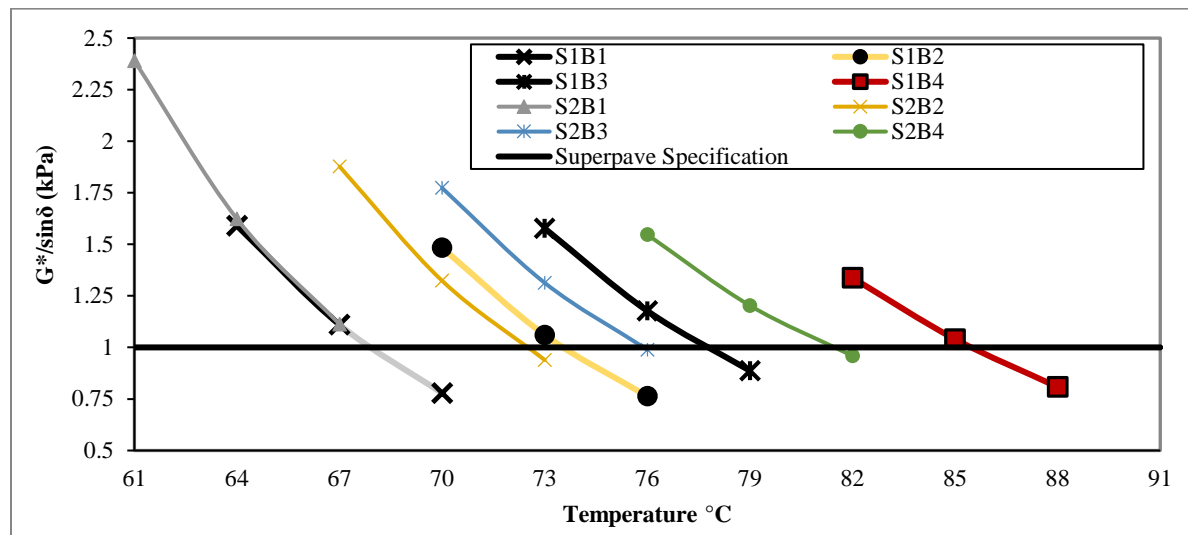


Figure 16.  $G^*/\sin\delta$  vs temperature (°C) curve for unaged S1 and S2 asphalt binders.

### 5.3. Multiple Stress Creep Recovery (MSCR)

The percent recovery (%R) values were higher for S1B4 and S2B4 binders than the others. As expected, the non-recoverable creep compliance ( $J_{nr}$ ) values were lower for these binders (PG 76-22) compared to the others. However, there was a little variation in test results between the PG

76-22 binders from two different sources (S1B4 and S2B4). The test results of the same PG binder from two different followed a similar trend. The overall results are shown in Figures 17 and 18.

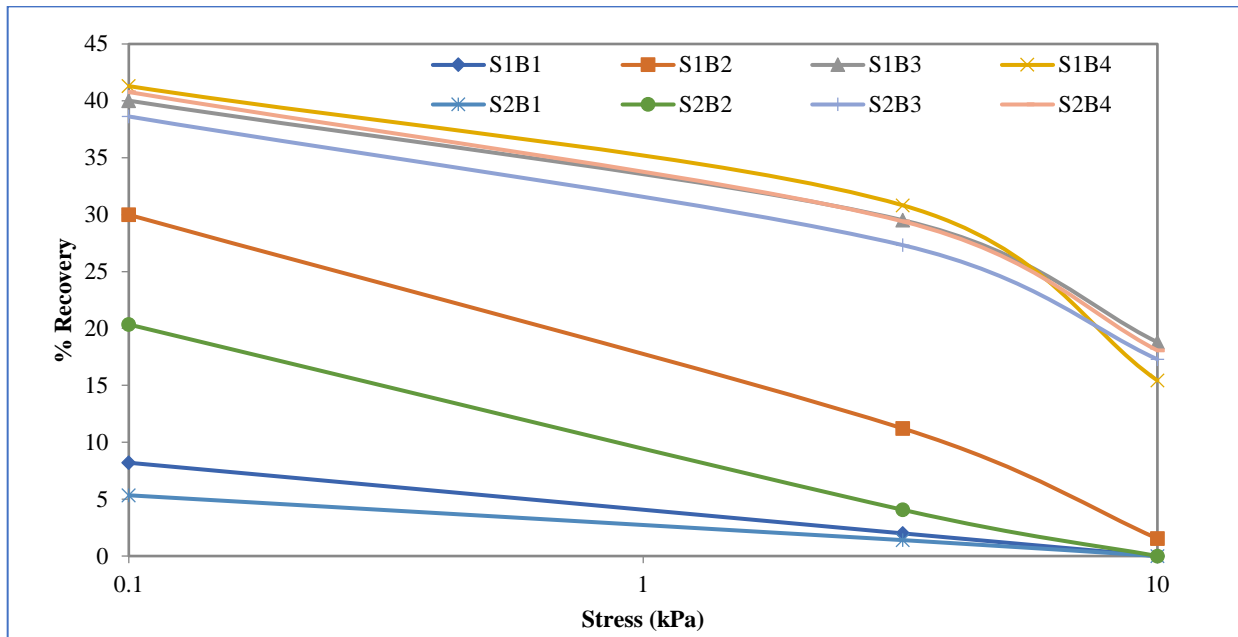


Figure 17. Percent recovery vs stress for source S1 and S2 asphalt binders.

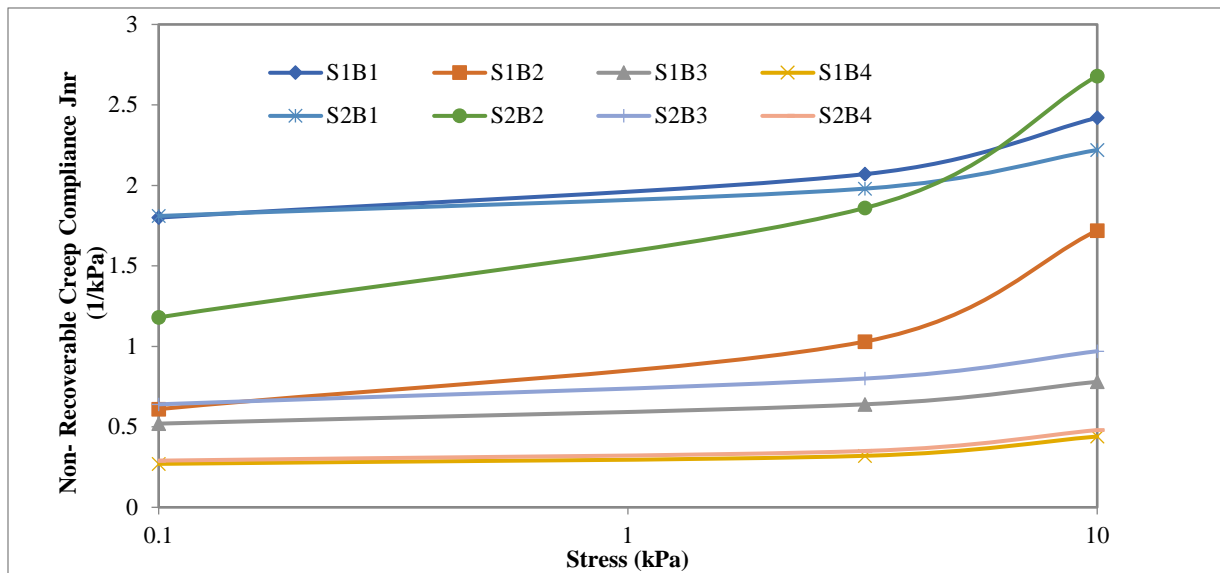


Figure 18. Non-recoverable creep compliance vs stress for source S1 and S2 asphalt binders.

Additional 16 binders were also evaluated by conducting the MSCR test, the percent recovery and non-recoverable creep compliance (Jnr) values of these binders are shown in Figures 19 and 20.

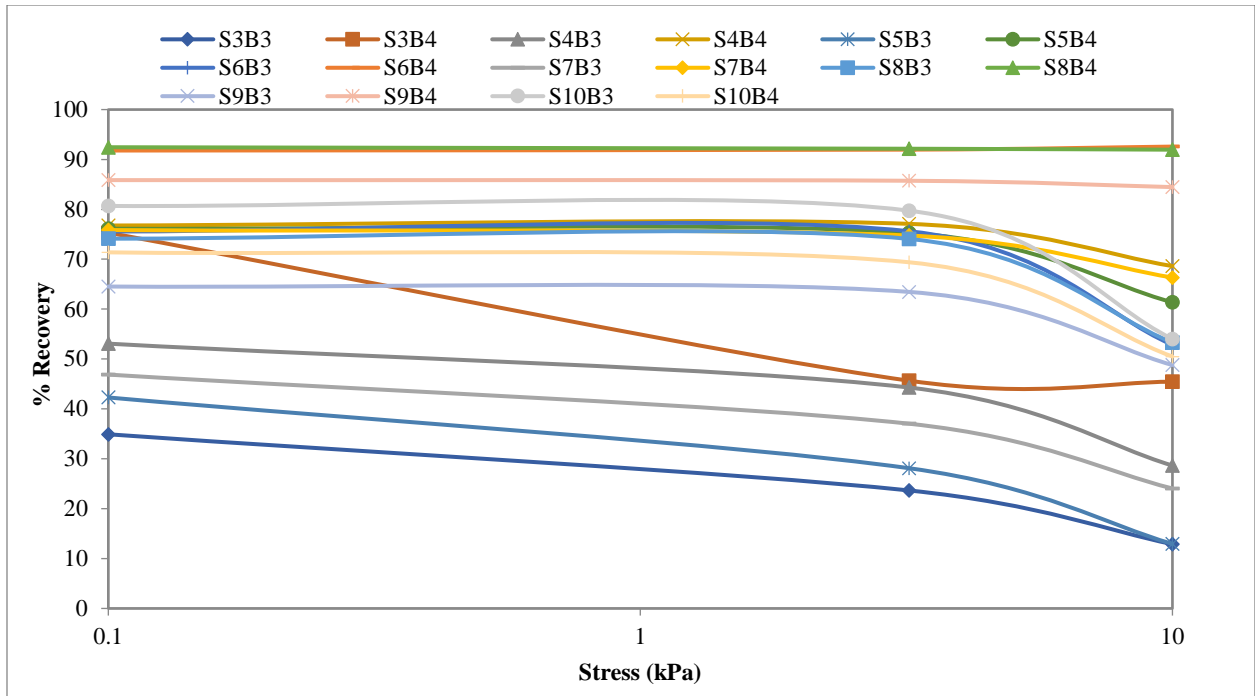


Figure 19. Percent recovery vs stress for additional modified asphalt binders.

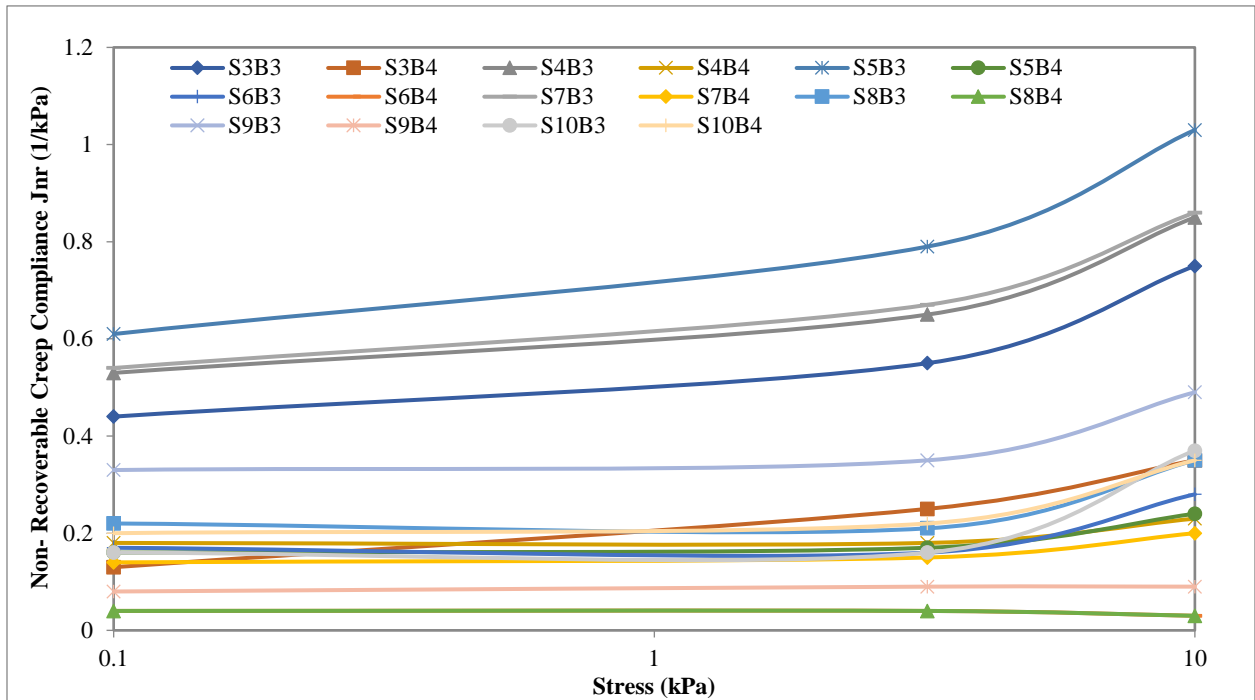


Figure 20. Non-recoverable creep compliance vs stress for additional modified asphalt binders.

### 5.4. Elastic Recovery test using DSR (ER-DSR)

The elastic recovery test was conducted using the DSR machine for both unaged and RTFO-aged modified asphalt binders. The temperature of the test sample was kept at the required 25°C for 20 minutes to reach thermal equilibrium. The ER-DSR test results for ARDOT-certified asphalt binders are shown in Figures 21 and 22. From the test results, it can be seen that modified binders have higher ER-DSR value compared to the unmodified binders. But the binders modified by PPA did not show higher ER-DSR value. Also, the tests results of ER-DSR are more repeatable. The ER-DSR test can identify the presence of polymeric modifiers.

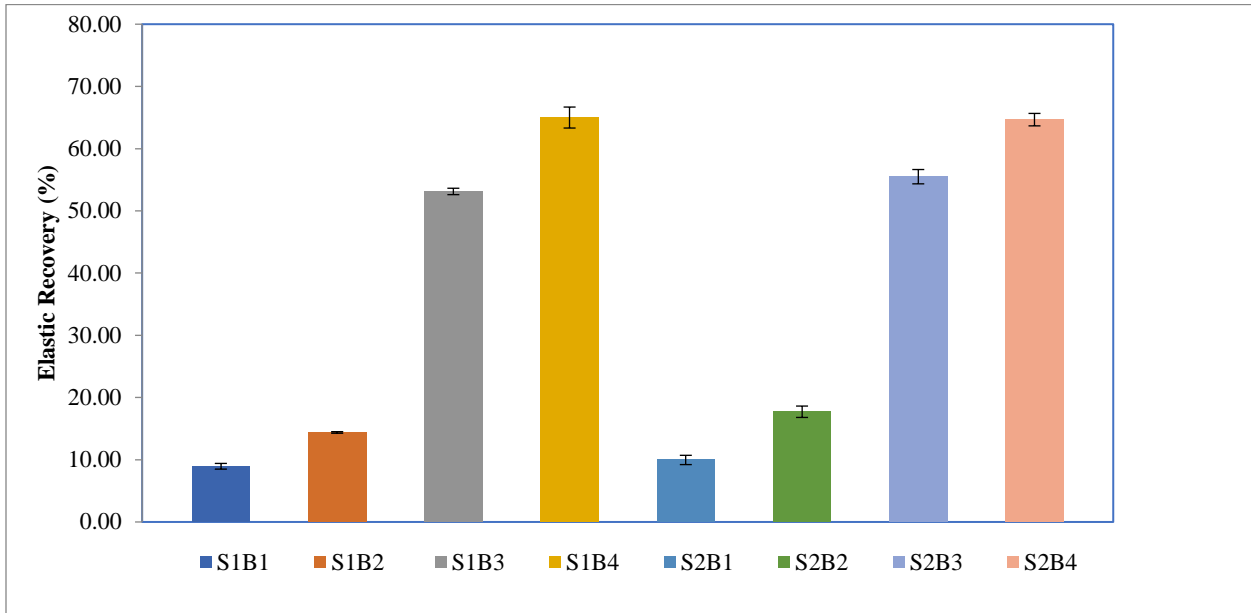


Figure 21. ER-DSR value for the ARDOT-certified unaged asphalt binders (source 1 and 2).

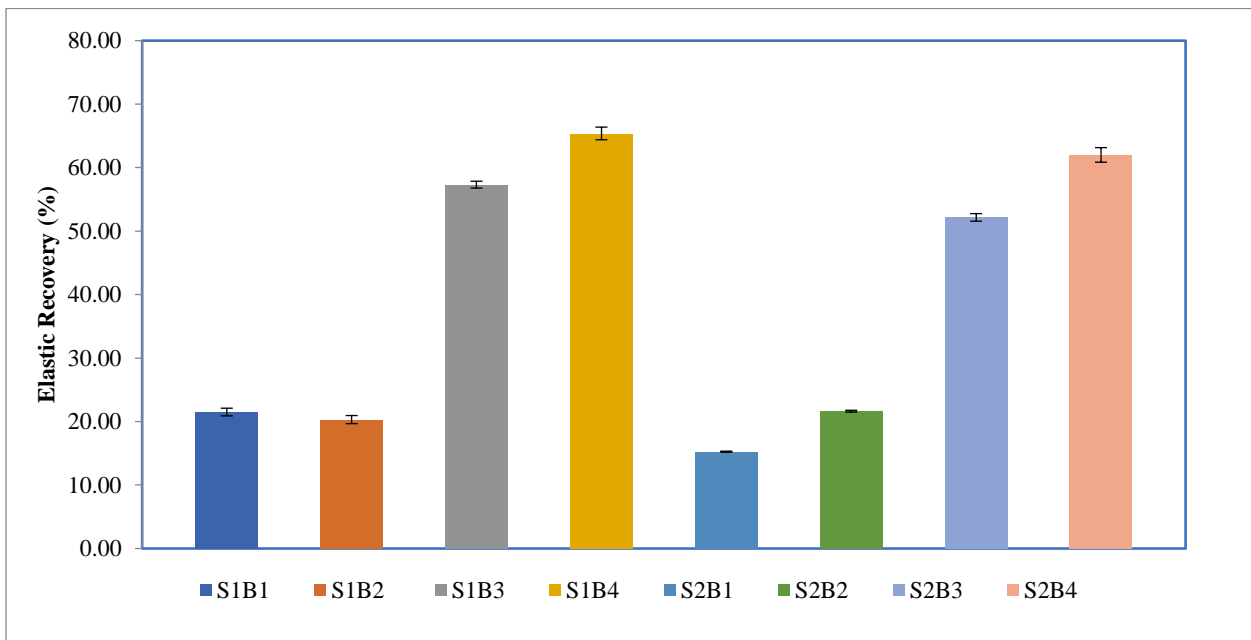


Figure 22. ER-DSR value for the ARDOT-certified RTFO-aged asphalt binders (source 1 and 2).

ER-DSR tests were also conducted on the modified asphalt binders from the other sources. Both unaged and RTFO-aged samples were tested, and test results are shown in Figures 23 and 24. Higher grade modified binders PG 76-22 showed higher ER-DSR value compared to the PG 70-22 binders. For PG 70-22 binders, at least 40% elastic recovery was found, whereas at least 60% elastic recovery was found for PG 76-22 binders. There was no significant variation observed between the results of unaged and RTFO-aged binders. Some researchers (e.g., (3)) suggested that RTFO-aged binder should be used to conduct ER-DSR test. Therefore, both unaged and RTFO-aged test results were used to correlate with the ER values.

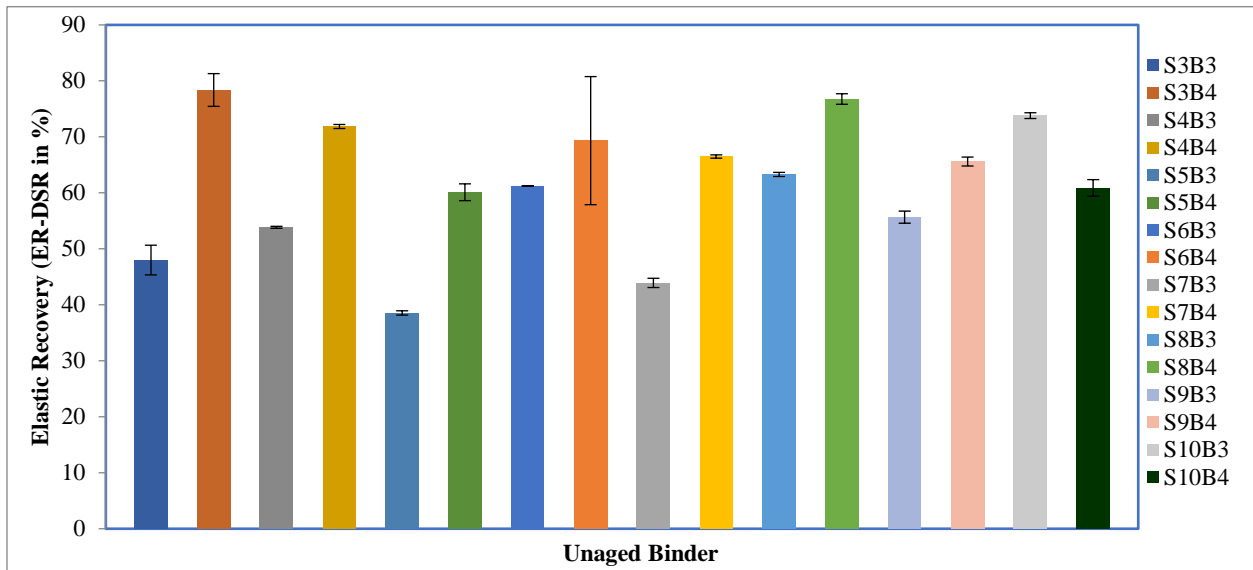


Figure 23. ER-DSR value for the additional unaged modified asphalt binders (source 3 to 10).

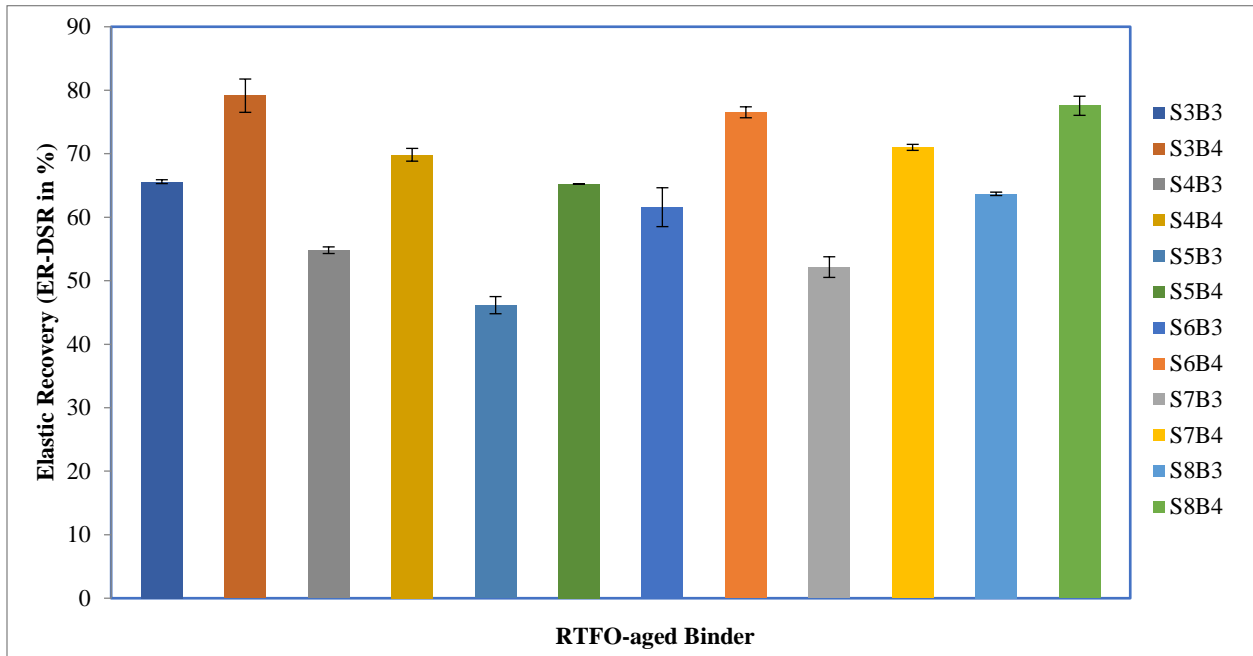


Figure 24. ER-DSR value for the additional RTFO-aged modified asphalt binders (source 3 to 8).

### 5.5. Binder Yield Energy Test (BYET)

The Binder Yield Energy Test (BYET) was conducted to determine the yield energy of the asphalt binders considered in this study. The RTFO-aged binders were used for testing and the test results are shown in Figures 25 and 26. The yield energy value was relatively very low for unmodified binders. Modified binders showed higher yield energy value while low yield energy was observed for PPA modified binders. Therefore, the presence of SBS can be identified through BYET but PPA could not be identified.

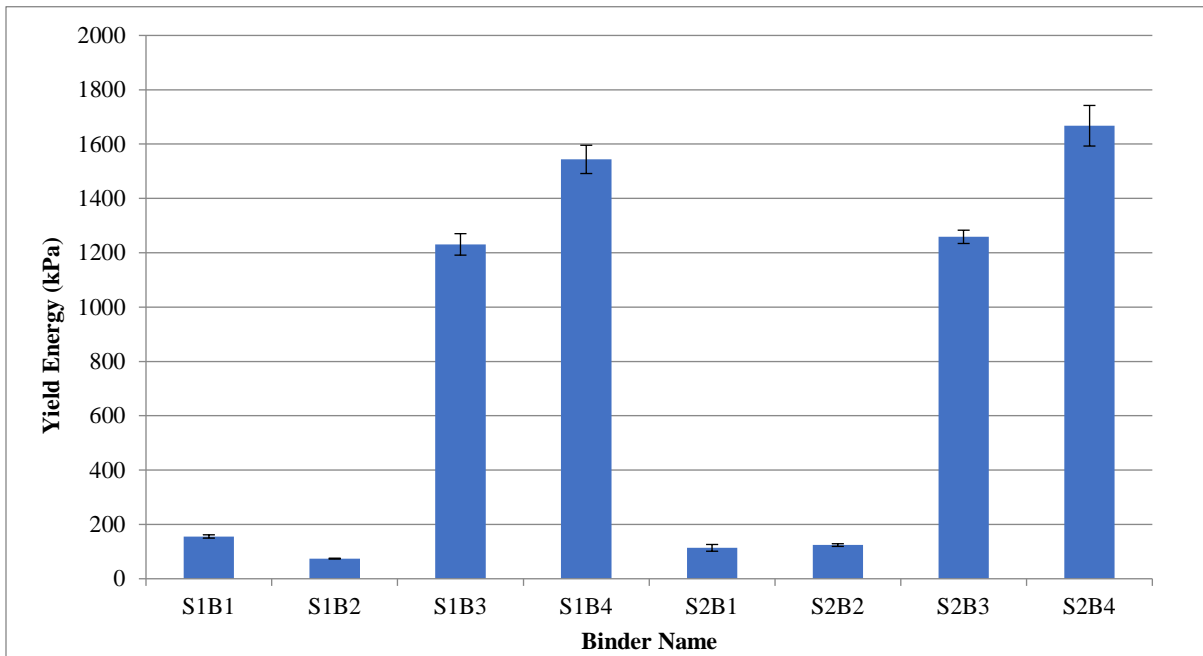


Figure 25. BYET value for the ARDOT-certified RTFO-aged asphalt binders (source 1 and 2).

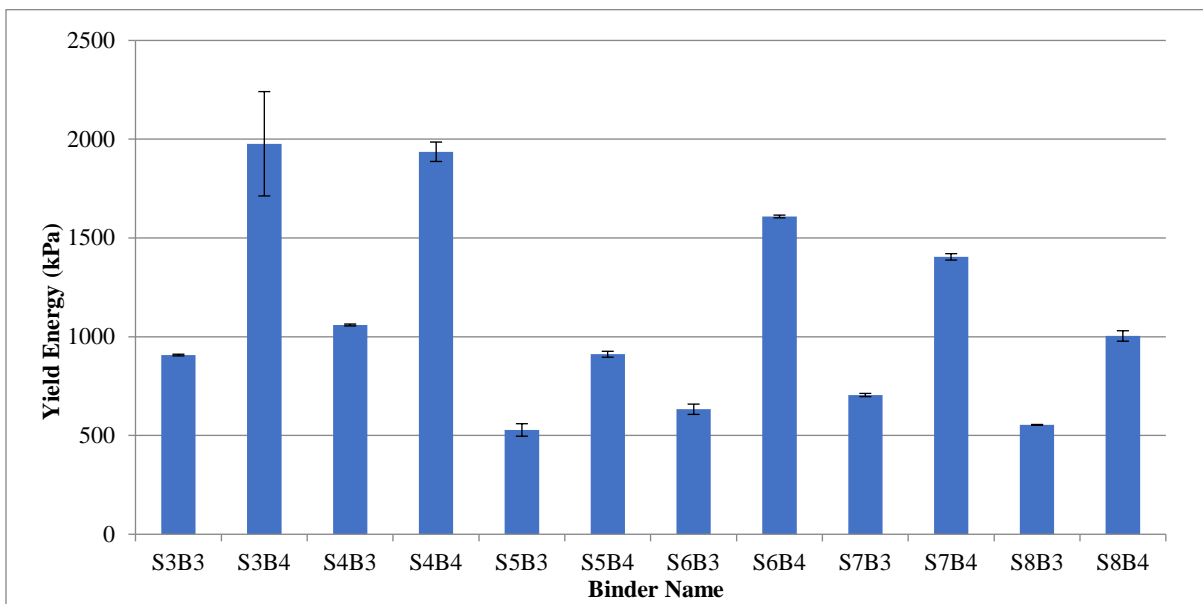


Figure 26. BYET value for the additional RTFO-aged modified asphalt binders (source 3 to 8).

## 5.6. Linear Amplitude Sweep (LAS)

Linear Amplitude Sweep (LAS) test was used to determine the fatigue resistance by applying cycle loading. Fatigue lives of the tested binders were calculated for strain levels of 2.5% and 5%. The LAS test results of the selected binders are shown in Figures 27 and 28. The number of cycles at 2.5% strain was found higher compared to the number of cycles at 5.0% strain. Also, no significant variation was observed between unmodified and modified binders. The LAS test can be used to characterize the damage accumulation. However, it cannot be used to identify the presence of polymers.

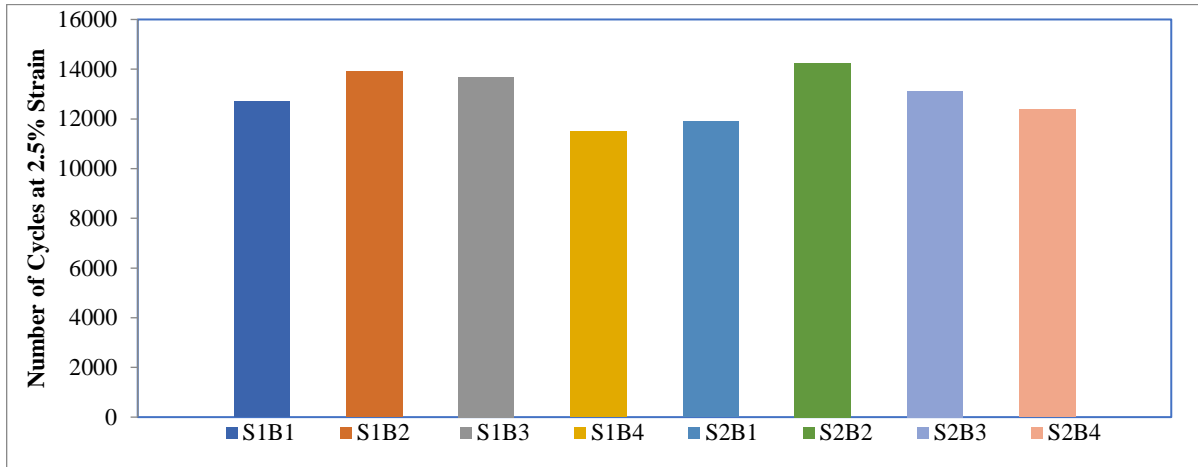


Figure 27. Number of cycles to failure at 2.5% strain for the ARDOT-certified PAV-aged asphalt binders (source 1 & 2).

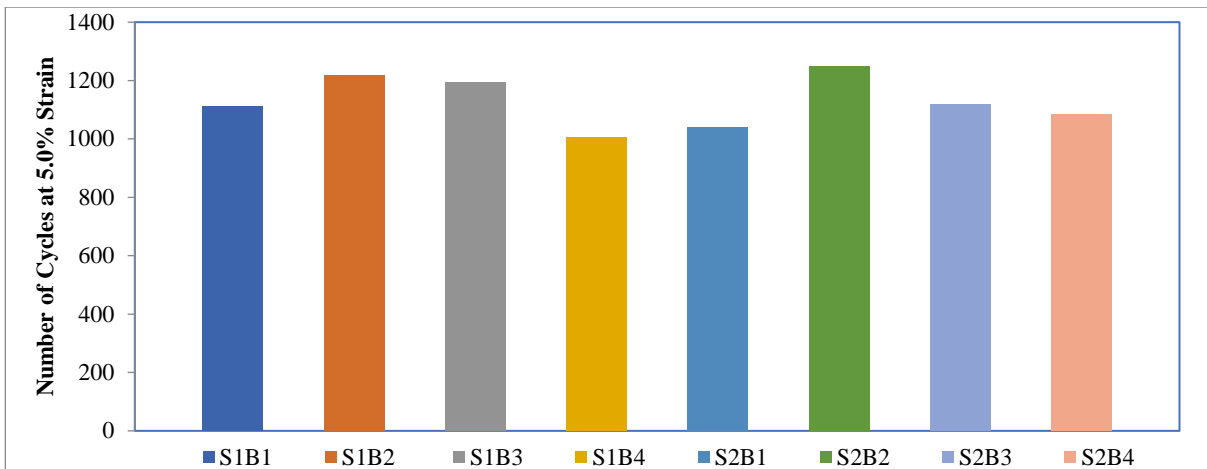


Figure 28. Number of cycles to failure at 5.0% strain for the ARDOT-certified PAV-aged asphalt binders (source 1 & 2).

## 5.7. Correlation between MSCR Percent Recovery (%R) Parameter and Elastic Recovery

The elastic recovery values were collected from the suppliers. The MSCR percent recovery (%R) values at 3.2 kPa were used for analysis. The main purpose of this analysis is to determine acceptable MSCR %R values for different PG binders so that the suppliers and users are not penalized for adopting new MSCR requirements. Figure 29 shows the relationship between the

MSCR percent recovery (%R) and ER values of PG 70-22 and PG 76-22 binders from different sources. A higher percent recovery was found for the higher elastic recovery asphalt binder. Figure 29 shows that the value of the variance ( $R^2$ ) is not relatively good to describe a good relationship between these two parameters. It can be concluded that 70% ER value correlates well with the 30% MSCR percent recovery value for PG 70-22 binder whereas, 80% ER value correlates well with the 50% MSCR percent recovery value for PG 76-22 binder.

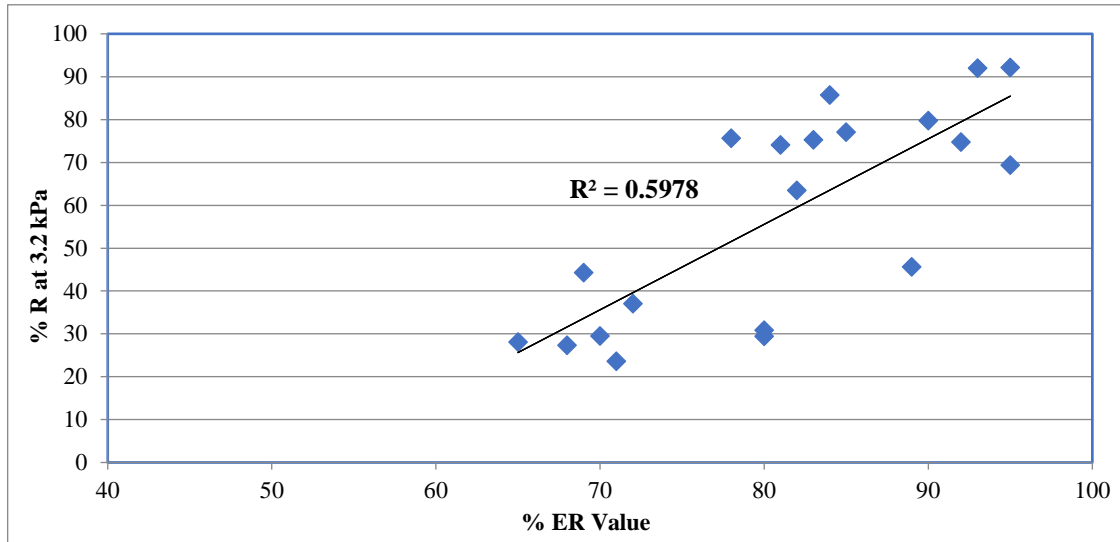


Figure 29. Correlation between MSCR percent recovery (%R) at 3.2 kPa and elastic recovery (AASHTO T 301).

### 5.8. Correlation between MSCR non-recoverable creep compliance ( $J_{nr}$ ) Parameter and Elastic Recovery

Another MSCR parameter, the non-recoverable creep compliance ( $J_{nr}$ ), has a good correlation ( $R^2=0.80$ ) with the elastic recovery value using the ductility bath shown in Figure 30. A lower  $J_{nr}$  value indicates higher elastic recovery of the PG Plus asphalt binder. In addition, the  $J_{nr}$  values are very low for ER values ranging from 80 to 90%. From Figure 30, it can be seen that a 70% ER value correlates well with the 0.5 (1/kPa) MSCR non-recoverable creep compliance value ( $J_{nr}$ ) for PG 70-22 binder, whereas, 80% ER value correlates well with the 0.1 (1/kPa) MSCR percent recovery value for PG 76-22 binder. It is still tough to suggest the  $J_{nr}$  value for 80 percent to 90 percent elastic recovery value due to the slight variation of data.



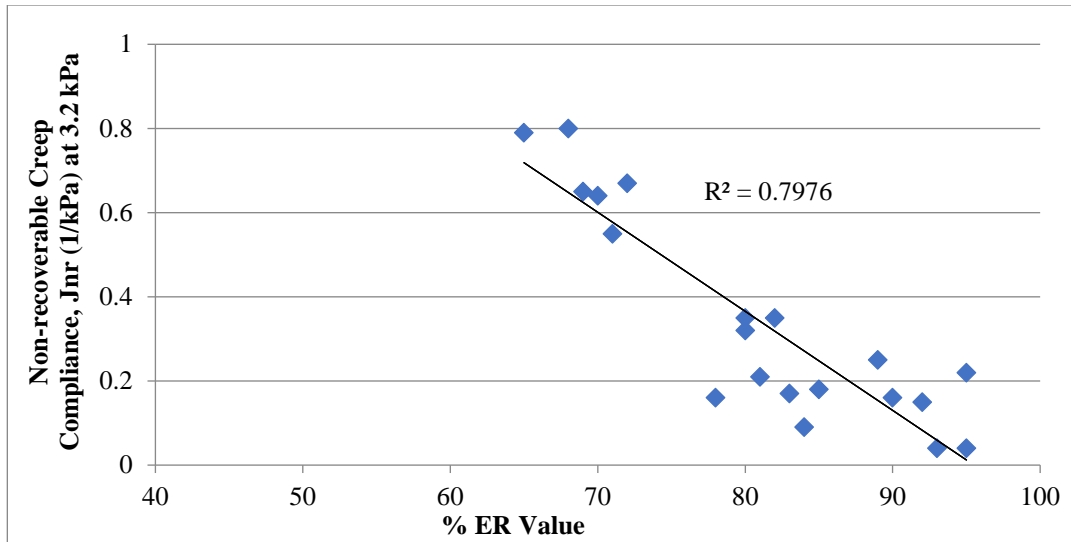


Figure 30. Correlation between MSCR non-recoverable creep compliance (Jnr) at 3.2 kPa and elastic recovery (AASHTO T 301).

### 5.9. Correlation between ER-DSR and ER

The elastic recovery using DSR (ER-DSR) test was conducted for unaged and RTFO aged modified asphalt binders. The correlation between the ER-DSR and elastic recovery using the ductility bath is shown in Figures 31 and 32. These figures have two test results of two types of binders from different sources; PG 70-22 binders' datapoints are on the left and PG 76-22 binders' datapoints are on the right. As seen from these figures, a better correlation was found between the ER-DSR and ER of RTFO-aged asphalt binders ( $R^2=0.85$ ) compared to the correlation between the ER-DSR and ER values for unaged asphalt binders ( $R^2=0.67$ ). The variation of the ER-DSR test results was possibly due to the mode of loading, strain rate, sample geometry, temperature control, and operator sensitivity. Besides, a shear load is applied in the DSR, while a tensile load is applied in the ductility bath. From Figure 31 and 32, it can be said that the 70% ER value correlates well with the 40% ER-DSR value for PG 70-22 binder whereas, 80% ER value correlates well with the 50% ER-DSR value for PG 76-22 binder. Due to the automated measurement, easy sample preparation and continuous monitoring of the test results, the ER-DSR would be a better replacement of the ductility bath-based ER test. Researchers also suggested that the relaxation time after loading for the ER-DSR test should be 30 minutes.

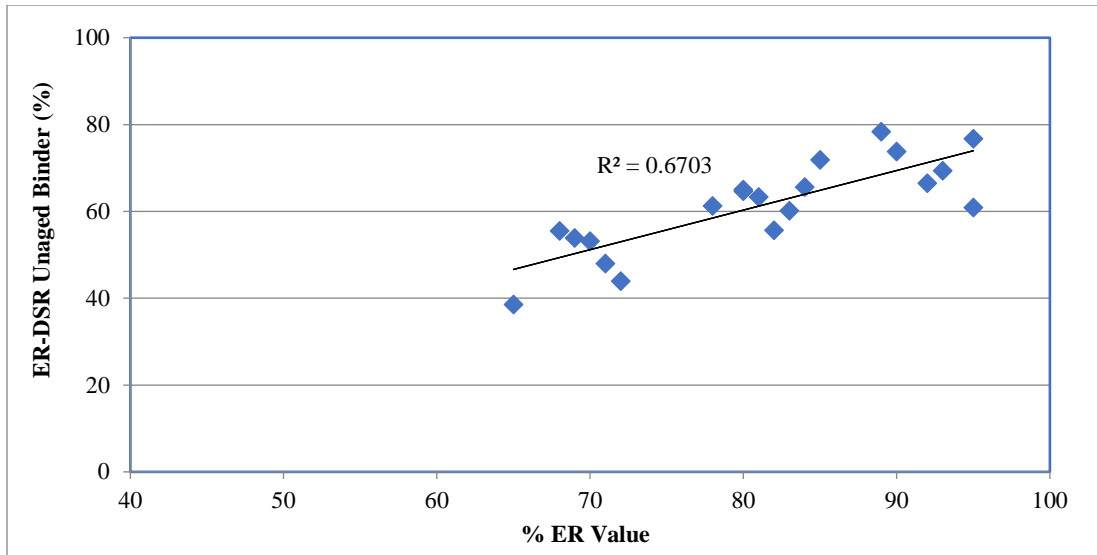


Figure 31. Correlation between ER-DSR (%) for unaged binder and elastic recovery (AASHTO T 301).

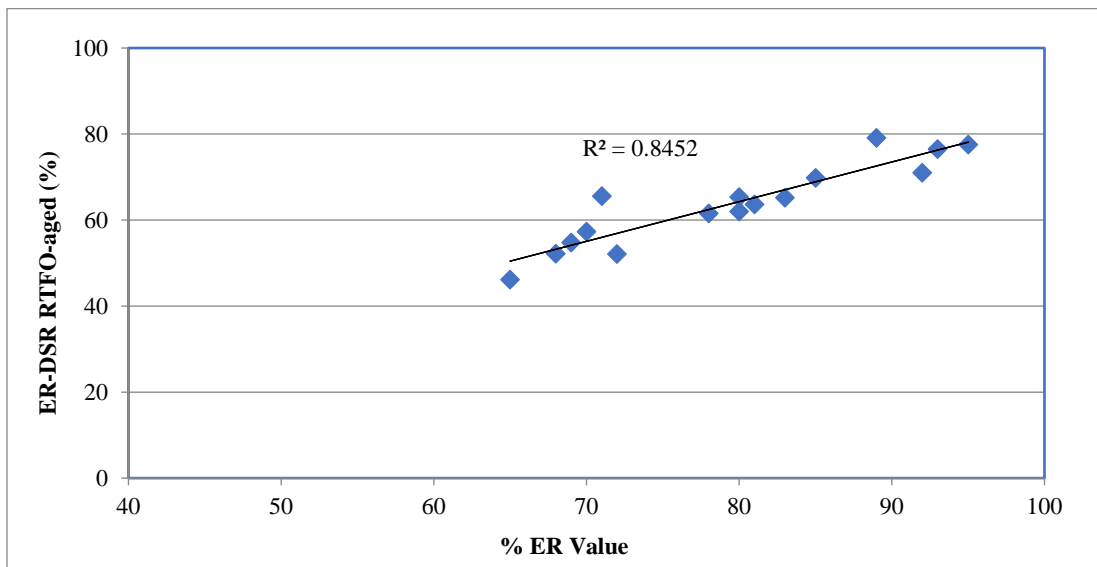


Figure 32. Correlation between ER-DSR (%) for RTFO-aged binder and elastic recovery (AASHTO T 301).

### 5.10. Correlation between the Binder Yield Energy Test (BYET) and Elastic Recovery

Figure 33 shows the correlation between the binder yield energy and elastic recovery using the ductility bath. A very poor relation ( $R^2=0.18$ ) exists between these two parameters. Figure 33 shows a lot of scattered data. Researchers used BYET as an indicator of fatigue cracking, but there is no relation to the existence of polymer. Therefore, the BYET is not recommended as an alternative to the ER.

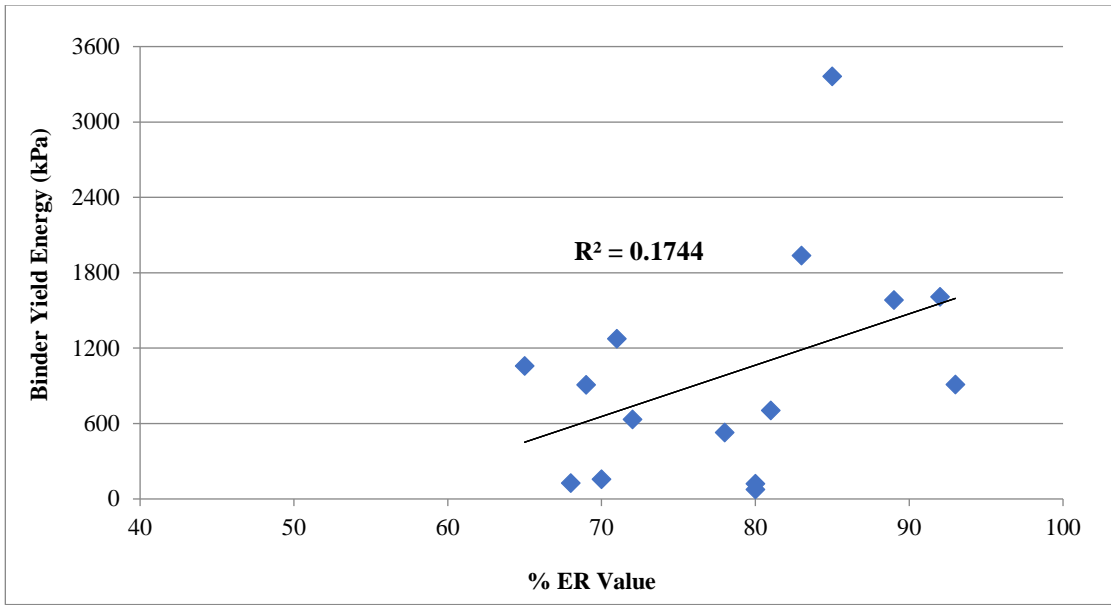


Figure 33. Correlation between the Binder Yield Energy Test (BYET) and elastic recovery (AASHTO T 301).

Another parameter strain at peak stress from BYET was used to correlate the elastic recovery data using the ductility bath as shown in Figure 34. However, a very poor correlation ( $R^2=0.0017$ ) was found between these two parameters. Theoretically, strain at peak stress represents an asphalt binder's ductility, but there is no relation with elastic recovery. So, BYET cannot be used to characterize the high-temperature properties of asphalt binders.

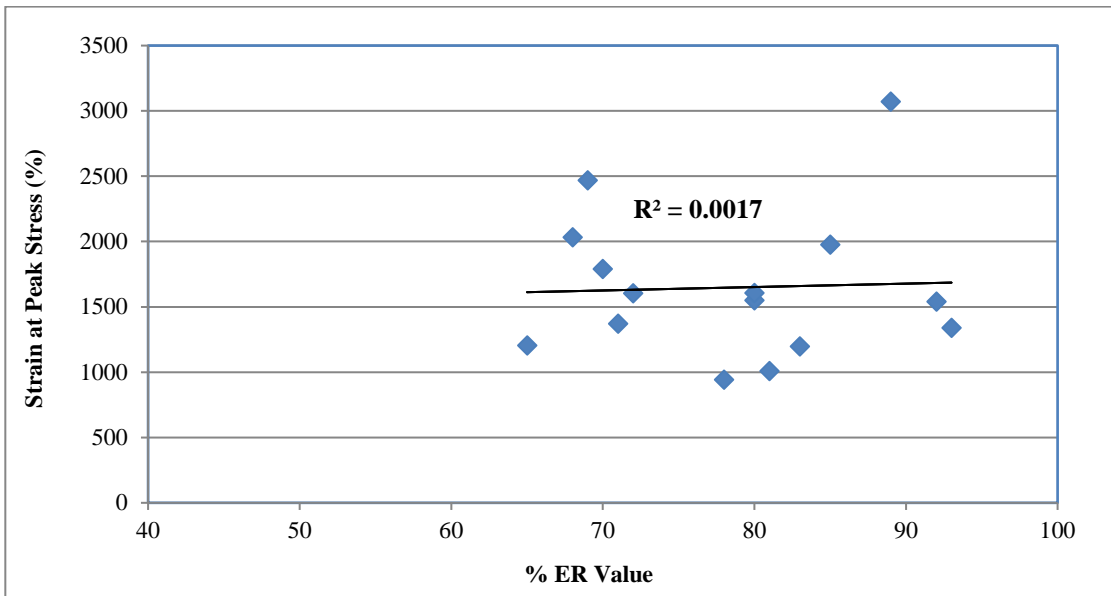


Figure 34. Correlation between the strain at peak stress from BYET and elastic recovery (AASHTO T 301).

Table 5 represents a summary of the correlations of elastic recovery using ductility bath (AASHTO T 301) with other parameters.

**Table 5. Summary and ranking of test parameters to replace elastic recovery (AASHTO T 301).**

<b>Alternative Test Method</b>	<b>Aging Condition</b>	<b>Test Name</b>	<b>Test Temperature</b>	<b>Justification</b>	<b>Rank</b>
ER-DSR	RTFO-aged	Elastic recovery using DSR (ER-DSR)	25°C	Correlates well, DSR based and simple	1
Non-recoverable creep compliance (Jnr)	RTFO-aged	Multiple Stress Creep and Recovery (MSCR)	64°C	Very good correlation and very simple	2
ER-DSR	Unaged	Multiple Stress Creep and Recovery (MSCR)	25°C	Good correlation and very simple	3
Percent Recovery (%R)	RTFO-aged	Elastic recovery using DSR (ER-DSR)	64°C	Good correlation, an indicator of the presence of the elastomer	4
Binder yield energy (BYE)	RTFO-aged	Binder Yield Energy Test (BYET)	25°C	Poor correlation	5
Strain at peak stress	RTFO-aged	Binder Yield Energy Test (BYET)	25°C	No correlation	6

From Table 5, it is seen that ER-DSR is the most effective and simplest test method to replace the elastic recovery using ductility bath (AASHTO T 301). Table 6 shows the recommended value of testing parameter against the three different values (70%, 80%, and 90%) of elastic recovery using ductility bath.

**Table 6. Recommended value of testing parameter against the value of elastic recovery using ductility bath (AASHTO T 301).**

<b>Performance Grade</b>	<b>Elastic Recovery (AASHTO T 301) Value</b>	<b>Corresponding ER-DSR value (RTFO-aged sample)</b>	<b>Corresponding Non-recoverable Creep Compliance (Jnr)</b>	<b>Corresponding ER-DSR value (Unaged sample)</b>	<b>Corresponding Percent Recovery (%R)</b>
PG 70-22	70%	40%	0.50 (1/kPa)	40%	30%
PG 76-22	80%	50%	0.10(1/kPa)	50%	50%
PG 76-22	90%	60%	0.05(1/kPa)	60%	60%

### 5.11. Relationship of ER-DSR with MSCR, and LAS Test Results

Figure 35 shows the relationship between the ER-DSR at 25°C and percent recovery (%R) from the MSCR test at 3.2 kPa for the asphalt binder. Good correlation was observed between these two parameters. It can be mentioned that the ER-DSR value of 20% was observed for the unmodified and PPA modified asphalt binders, and 50%, 60%, and 70% ER-DSR values were observed for the SBS and SBS+PPA modified asphalt binders. The presence of PPA cannot be determined by any DSR based tests. Thus, some chemical tests are being used in this study to identify the presence of PPA.

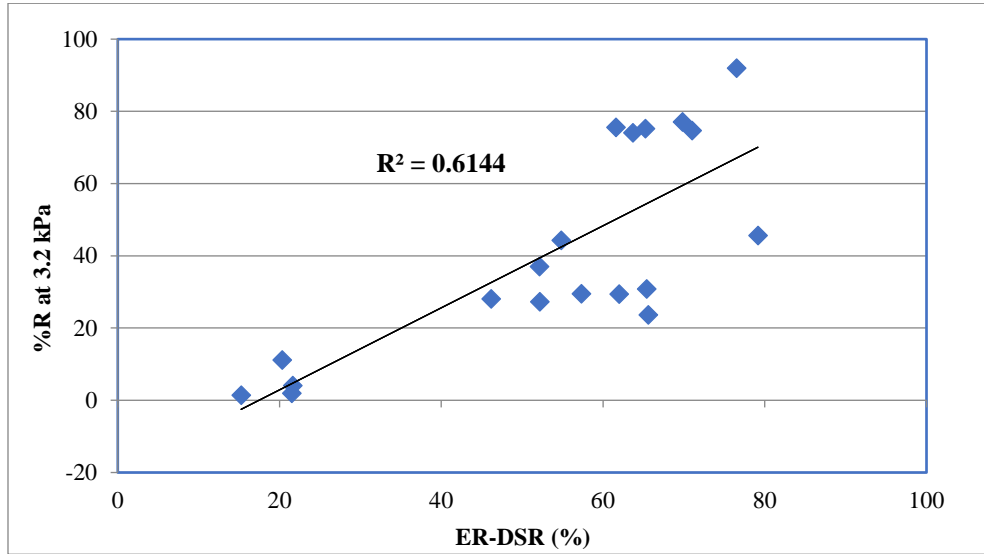


Figure 35. Correlation between MSCR percent recovery (%R) at 3.2 kPa and ER-DSR.

The correlation of the ER-DSR at 25°C with the number of cycles ( $N_f$ ) at 2.5% and 5.0% strain from LAS test are shown in Figures 36 and 37. However, a very poor relation exists with the ER-DSR test. Therefore, there is no scope to recommend ER-DSR test to predict fatigue resistance of asphalt binders.

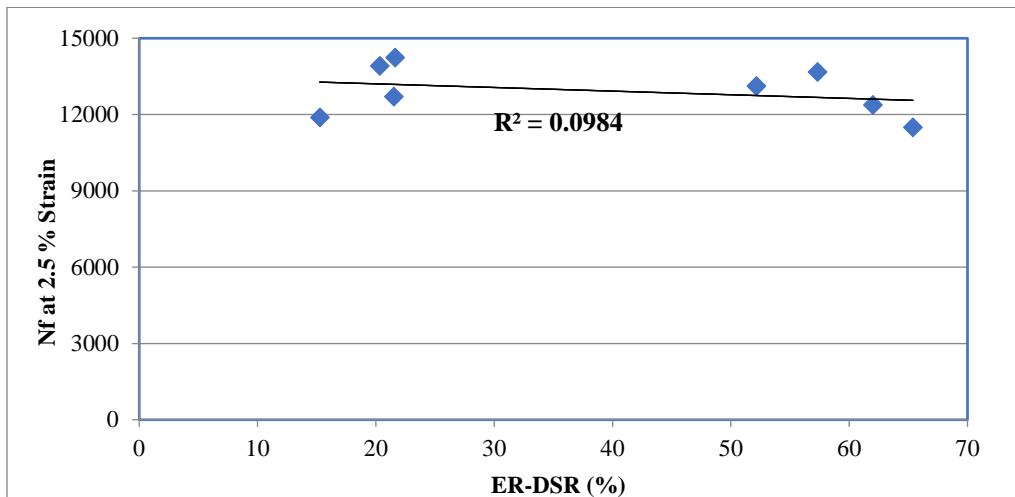


Figure 36. Correlation between number of cycles ( $N_f$ ) at 2.5% strain and ER-DSR.

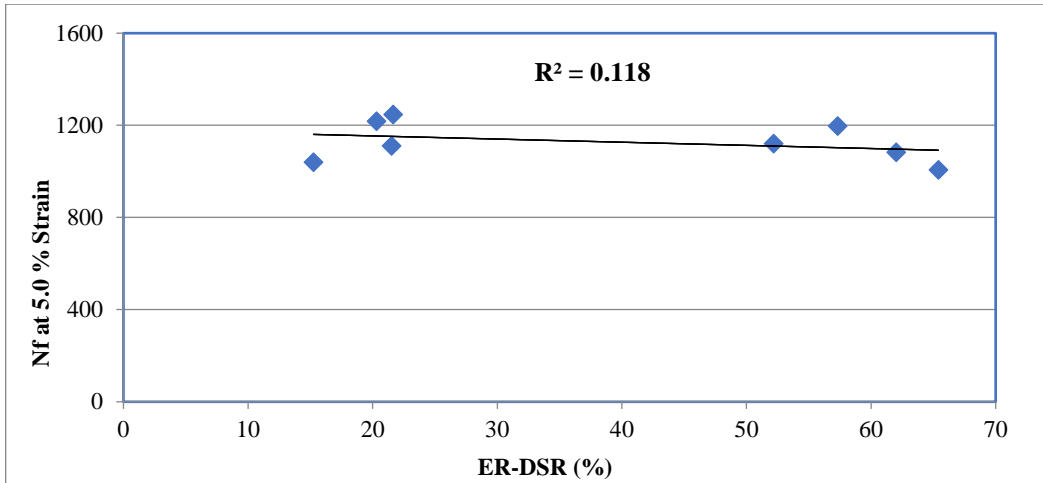


Figure 37. Correlation between number of cycles ( $N_f$ ) at 5.0% strain and ER-DSR.

### 5.12. pH Measurement

From pH measurement test results (Figure 38), it is observed that the unmodified binders from the respective sources are more acidic in nature than the modified binder samples. It is anticipated that the samples modified with PPA showed lower pH values than other samples. Even the samples modified with SBS had lower pH than the unmodified samples which indicates that the modification with PPA or SBS or both increases the polar fractions within the asphalt binders. As the stiffness of an asphalt binder sample increases with its polarity (34), pH measurement test can be used as a quick tool to compare the stiffness among multiple asphalt binder samples. Though pH measurement does not tell too much about the asphalt chemistry, it helps to trace the presence of acid and degree of modification.

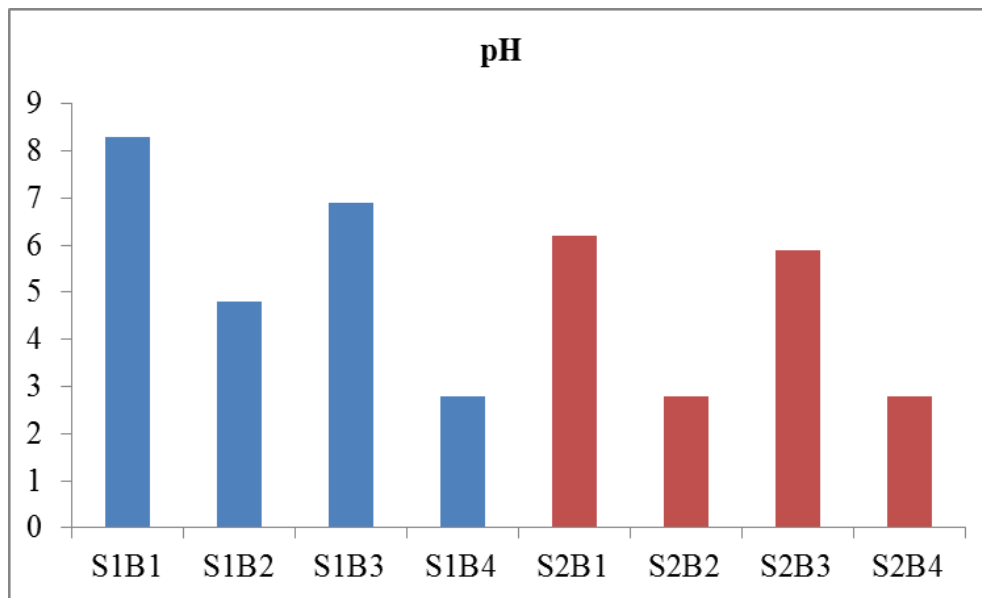


Figure 38. pH test results.

### 5.13. SARA Analysis

The SARA fractions result for unaged binders are shown in Figure 39. Asphalt binder samples from the Canadian crude source (Source-1) were found to be higher in Asphaltenes content than those from the Arabian crude source (Source-2). Even though both binders were from the same grade of PG 64-22 the neat binder from Source-2 (S2B1) had a different Asphaltenes content (13.2%) than the neat binder (S1B1) from Source-1 (19.9%). On the other hand, S1B1 binder had a low polar fraction (Resins) compared to S2B1. Binders modified with 0.5% PPA and 2% SBS (S1B4 and S2B4) had higher percentages of Asphaltene contents among unaged binders.

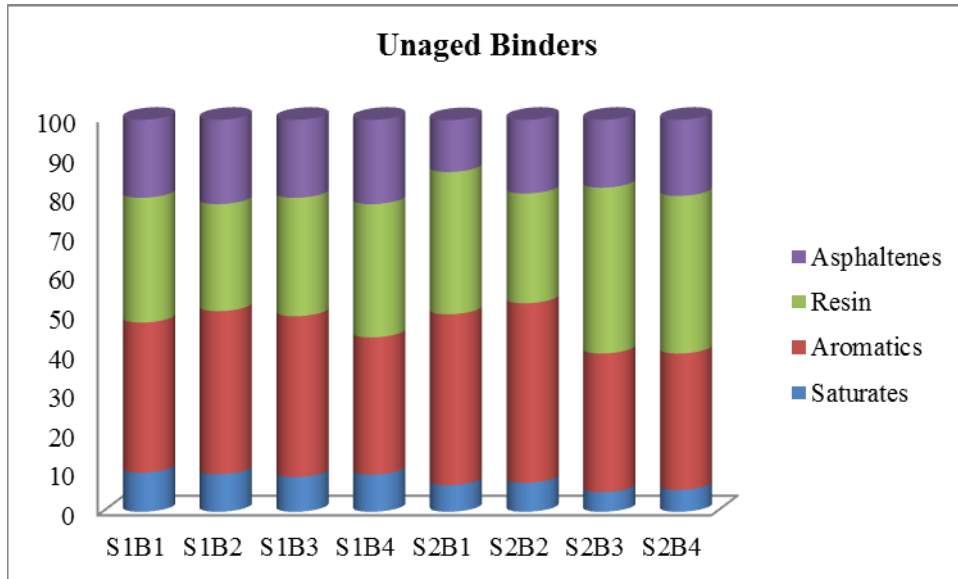


Figure 39. SARA fractions for unaged binder samples.

The SARA fractions for the RTFO-aged binders are reported in Figure 40. These samples showed increased percentages of Asphaltenes content after short-term aging in the case of both binder sources. The changes in other fractions did not follow any specific trend except the decreased Saturate contents. Like the unaged binders, unmodified binders (S1B1 and S2B1) had the lower percentages of Asphaltene contents whereas samples modified with 0.5% PPA and 2% SBS (S1B4 and S2B4) had higher percentages of Asphaltene contents among RTFO-aged binders.

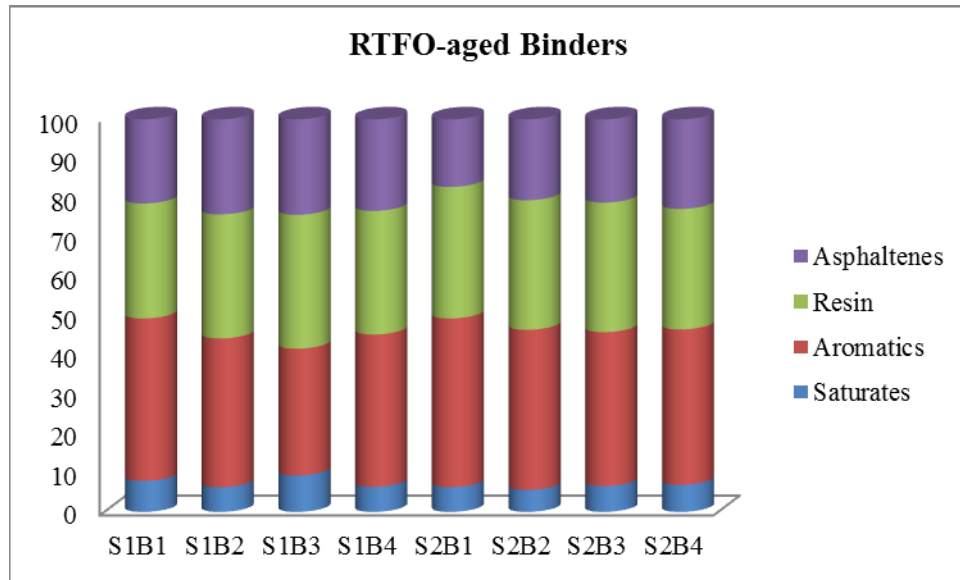


Figure 40. SARA fractions for RTFO-aged binder samples.

The SARA fractions for the PAV-aged binders are reported in Figure 41. Asphaltenes content rose significantly after PAV aging whereas Saturates were observed to decrease more. The Asphaltenes were found to follow a similar trend after PAV aging. Just like the unaged and RTFO aged binders, unmodified PAV -aged binders (S1B1 and S2B1) exhibited the lower percentages of Asphaltene contents whereas samples modified with 0.5% PPA and 2% SBS (S1B4 and S2B4) exhibited higher percentages of Asphaltenes.

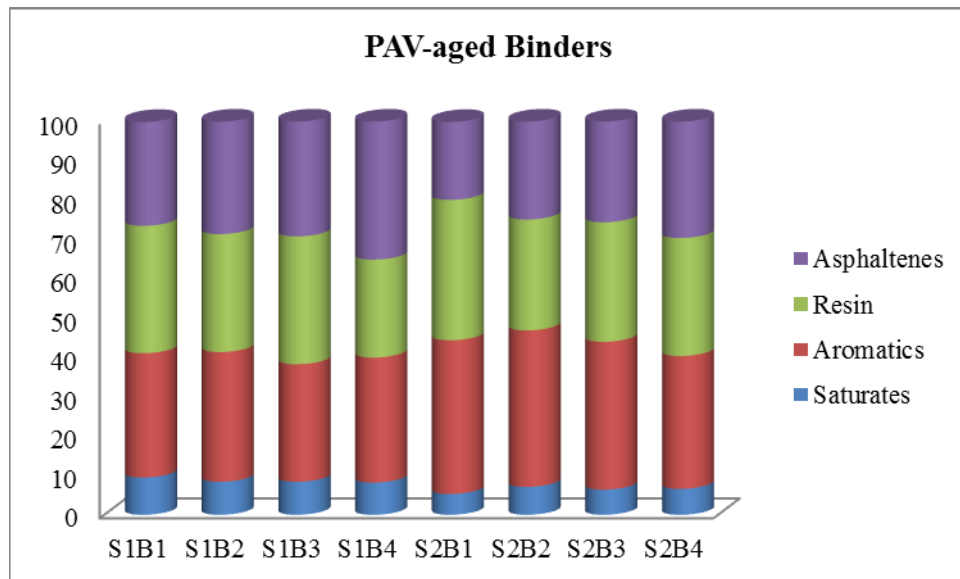


Figure 41. SARA fractions for PAV-aged binder samples.

SARA fractions can be used to evaluate the colloidal stability of the asphalt binder. Among the four chemical fractions of asphalt binders, Asphaltenes are highly polar and remain dispersed in a system consists of Aromatics and Resins. The solubility of Asphaltenes in the medium of Aromatics and Resins is the key factor of the colloidal stability of the binder which is measured



by Gaestel Index (22). Binder with too high Gaestel Index tends to be harder and colloiddally unstable (sooner to cause fatigue) whereas, a binder with too low Gaestel Index tends to be softer and unstable too. That's why binder with Gaestel Index within an intermediate range (22) is accepted for a practical purpose. Gaestel Index for all the samples remained within the anticipated range which ensured that the samples are colloiddally stable (Figure 42). Thus, SARA analysis can be used to predict fatigue. Moreover, mechanistic properties like viscosity and rutting parameters are highly correlated with the SARA fractions (35). So, SARA analysis can be used as a tool to find out the required extent of chemical modification for ensuring a certain level of mechanistic properties.

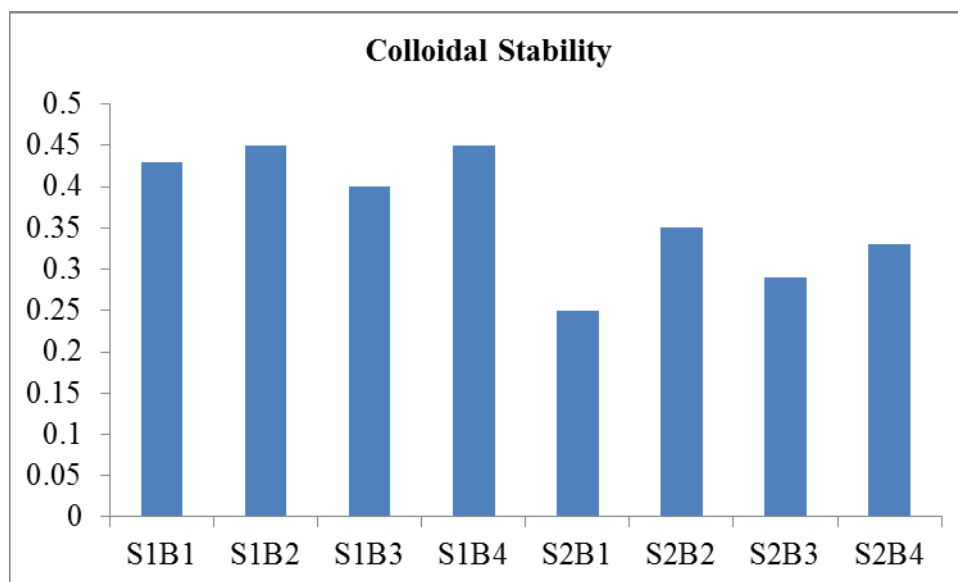


Figure 42. Gaestel Index (I<sub>c</sub>).

#### 5.14. NMR Analysis

NMR tests were conducted on separated asphalt fractions for their purity. The Saturates fraction was found to be more distinguishable. But there was a possibility of error of being eluted as one another as molecular structures of Aromatics and Resins are very similar. Aromatics have ring structures with some heteroatoms, whereas Resins are the amalgamation of many similar Aromatics compound with more heteroatoms. For clarification of the separated fractions, <sup>1</sup>H NMR was conducted on these two fractions only. A distinctive peak was found for the Aromatic fractions with the Resins between 2-4 ppm. The peak emerged due to Sulfur (S) atoms attached to the structure. The peaks between 0 and 2 were for -CH<sub>3</sub>, and -CH<sub>2</sub>, respectively. The area integral beneath the curve between the peaks 2 and 4 was taken as 1.000 and the other integrals were measured accordingly. It was observed in Figures 43 and 44 that the peaks between 2 and 4 increased, which is a clear indication of increased S atoms which were attached to the separated Resins fraction. Moreover, reduced peaks between 0 and 2 indicate the reduction of the -CH<sub>3</sub>, -CH<sub>2</sub> groups which got fused in Aromatics ring and formed larger cyclic structures of Resins.

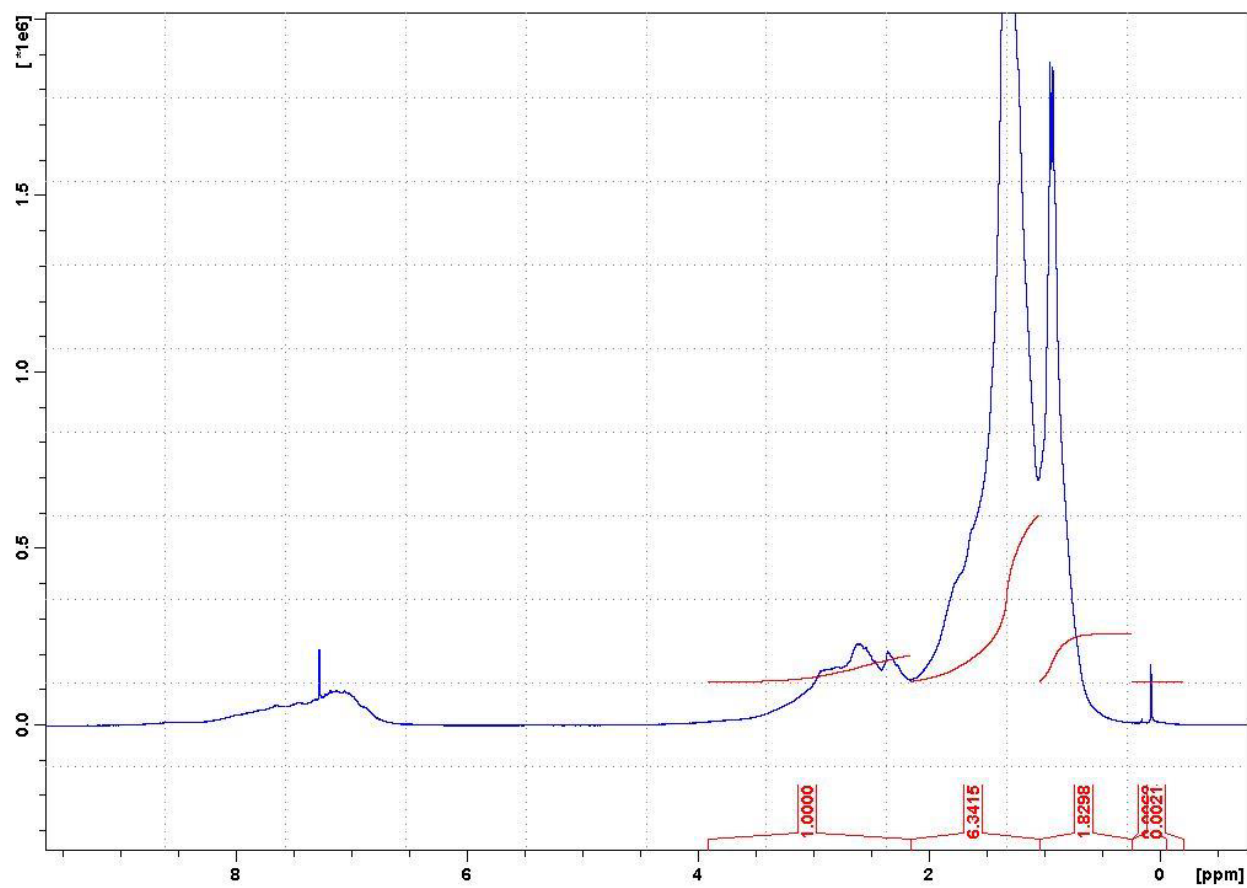


Figure 43. Typical NMR spectra for the aromatic compounds.

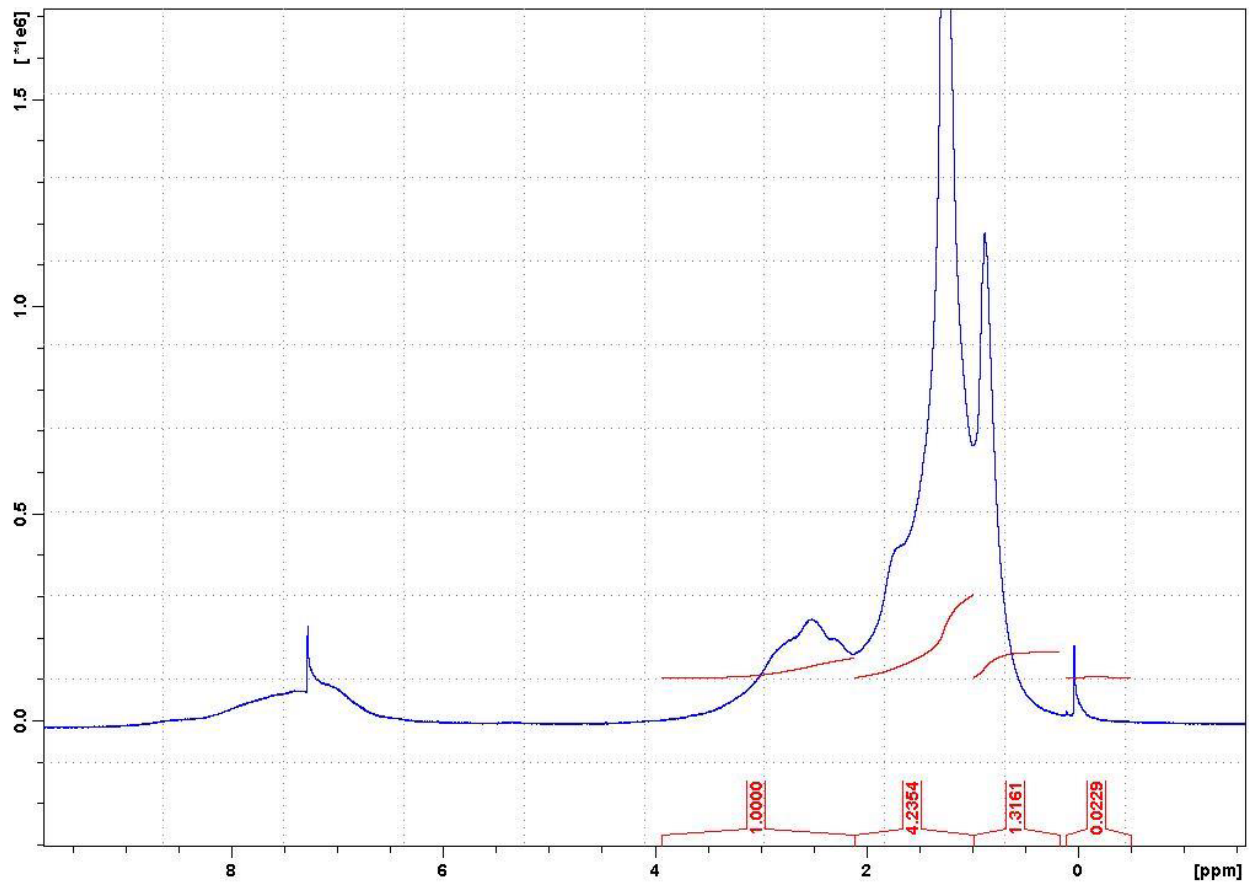


Figure 44. Typical NMR spectra for the resins compounds.

### 5.15. FTIR Analysis

In general, from the FTIR spectra of SBS and PPA modified asphalt binders, it was evident that neither of the modifiers added any new functional group to the binder samples, rather only showed some variation in absorbance for some specific wavenumbers. These variations may occur due to the oxidation reactions during aging or interactions between modifiers and binder components. Some significant modification was observed in chemical bonding before and after RTFO and PAV aging. The change in bonding ratios for the asphalt binder samples before and after RTFO and PAV aging are shown in Figures 45, 46, 47, 48, 49 and 50.

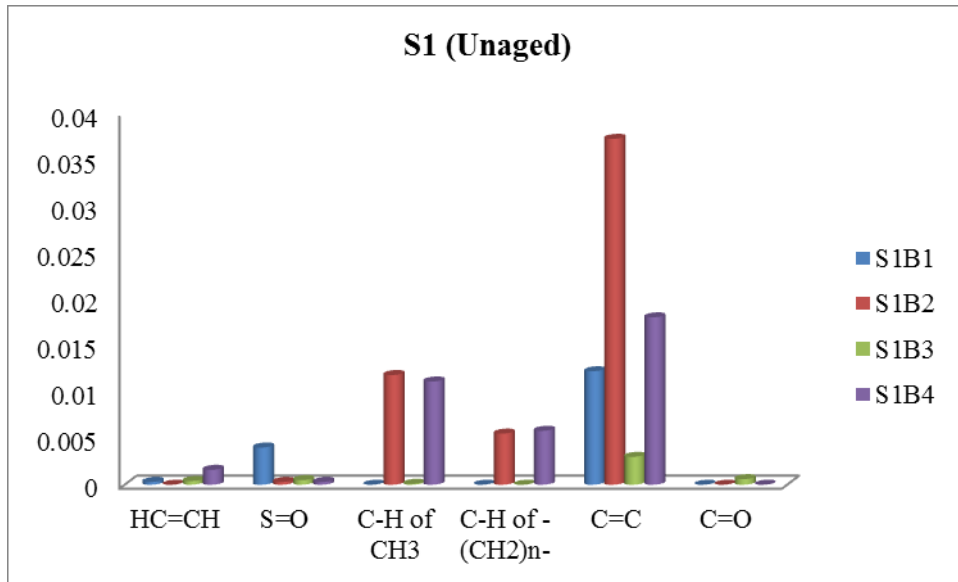


Figure 45. Ratio of bonding for source 1 (unaged) binders.

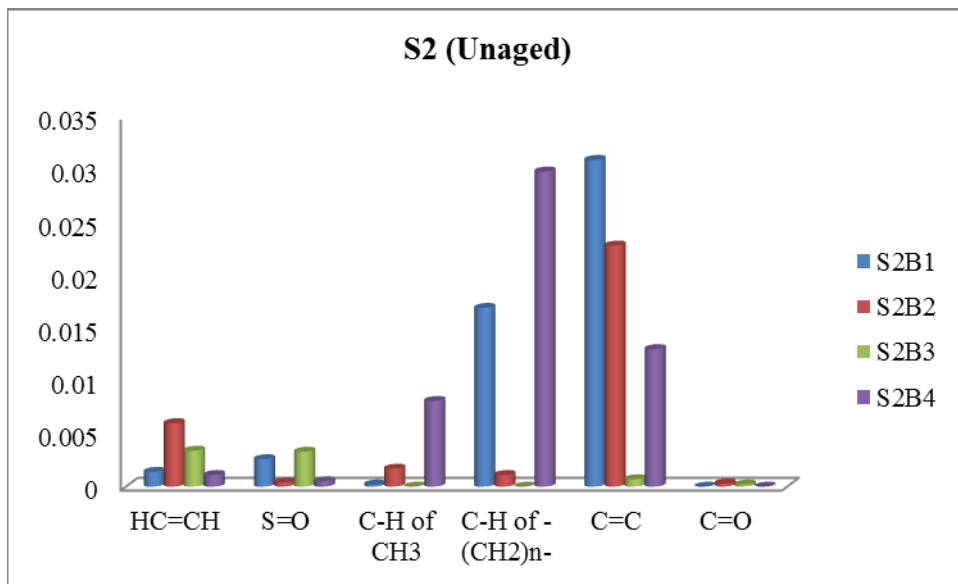


Figure 46. Ratio of bonding for source 2 (unaged) binders.

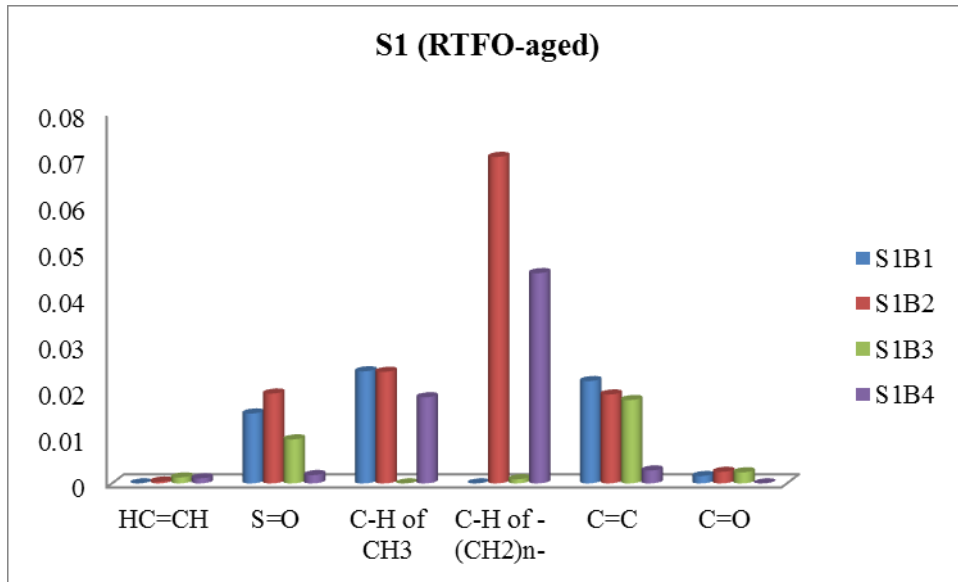


Figure 47. Ratio of bonding for source 1 (RTFO-aged) binders.

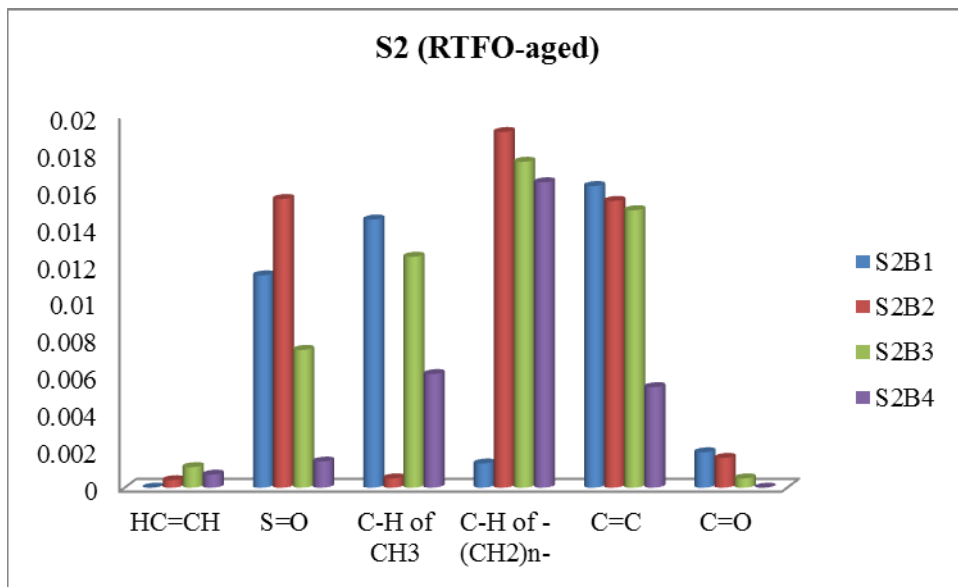


Figure 48. Ratio of bonding for source 2 (RTFO-aged) binders.

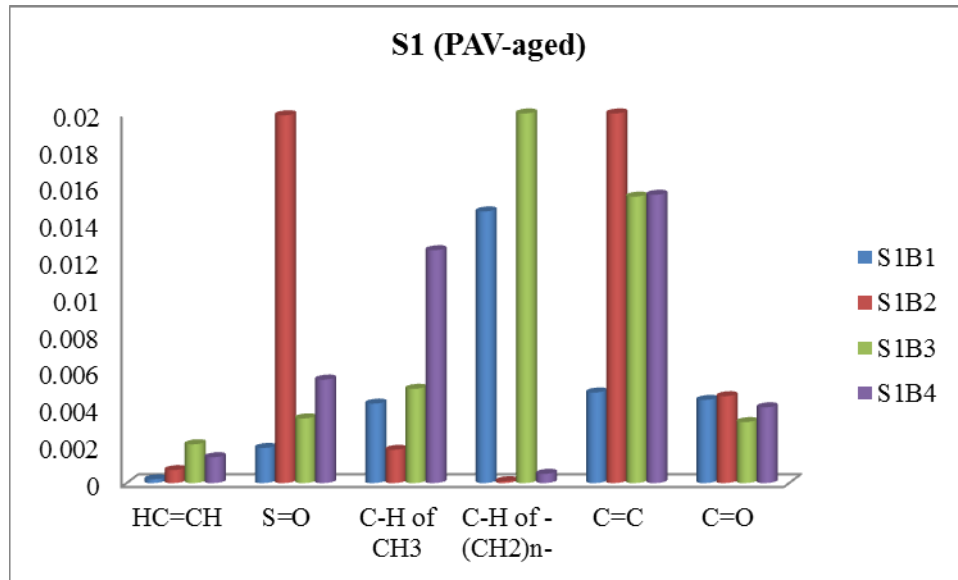


Figure 49. Ratio of bonding for source 1 (PAV-aged) binders.

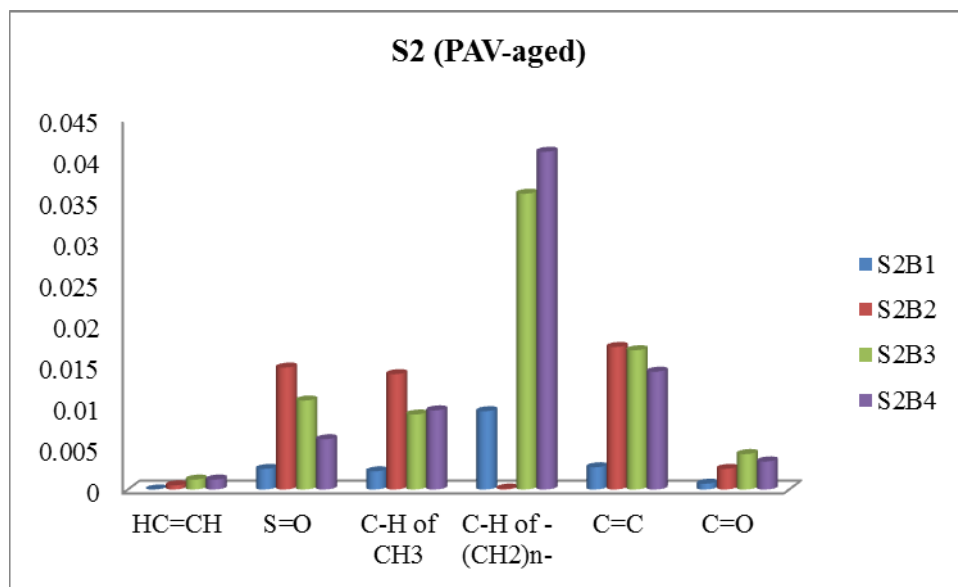


Figure 50. Ratio of bonding for source 2 (PAV-aged) binders.

A significant change was observed in near the ethylene band (HC=CH) mostly due to SBS modification. During the aging process in the asphalt binders, butadiene index values had decreased significantly due to the interaction between SBS and base binders which is more observable for Source 2 binders. Significant changes were also be observed in the sulfoxide index (S=O), which also increased after RTFO and PAV aged samples. The reason for increasing bonding ratio can be the attachment of oxygen molecule from the air with the binder during aging (36). While exposed in the field condition, oxygen molecules in the air weakens the weaker bonding in the asphalt molecule and transform into carbon-dioxide and water by the oxidation process. Aromatics are hydrocarbons with planar structure and can be characterized by double or single bonds with carbon rings stacked over each other, whereas, aliphatic compounds

are a non-planar structure with single carbon bonds without any stacking. These differences in chemical structures occur the difference in properties of aromatics and aliphatics (37). During the aging reactions in the asphalt binder, aromatic index ratios were observed to ratio increase whereas aliphatic index ratios were observed to decrease overall. Aging occurs in the presence of sunlight, heat, and air which contain oxygen. Under these circumstances, maltene fractions converted into aliphatic hydrocarbons which eventually reacted with the oxygen to form insoluble asphaltenes. During the aging process of asphalt binder, Resins and Asphaltenes contents interact with oxygen from air transformed into aromatic or aromatic hydrocarbons. That's why, after subsequent aging reactions, an increased ratio of the aromatic index (C=C) was observed. The carbonyl index indicates the extent of oxidation in the asphalt binder. From Figure 47 and 48, it is evident that the carbonyl index (C=O) varied after RTFO aging process. The parameter increased significantly (Figure 49 and 50) after the PAV aging process for both Source 1 Source and 2 binders.

There are some significant co-relations found after combining the SARA analysis and FTIR test results. Firstly, unmodified binders were found to have a high aromatic index (concentrated near  $1600\text{ cm}^{-1}$ ) than the modified binder samples. This parameter is found to decrease gradually after aging which is due to decreased Aromatics in RTFO and PAV binder samples. Secondly, samples modified with SBS were observed to have a higher ethylene index (concentrated near  $966\text{ cm}^{-1}$ ) than other samples. Some researchers found a significant peak for butadiene index near similar wavenumbers which can result in this higher index value for HC=CH. Finally, samples with higher Asphaltene contents exhibited higher aliphatic index (concentrated near  $1376\text{ cm}^{-1}$  and  $1460\text{ cm}^{-1}$ ) which eventually found to have higher viscosity and rutting parameter. As mechanical properties are found to be correlated with chemical composition, it is expected that with further study FTIR test can be used to compare certain properties (e.g., viscosity and rutting parameter) of asphalt binders. Moreover, some variation can be observed in the samples due to aging. Therefore, FTIR test can be used as a quick tool to evaluate the change in chemical fingerprint due to aging.

## 6. CONCLUSIONS

Different ARDOT-certified PG asphalt binders were tested in the study. The efficacy of DSR-based MSCR, ER-DSR, BYET, and LAS tests were evaluated as an alternative of the elastic recovery (ER) test method using a ductility bath (AASHTO T 301). Based on the test results the following conclusions could be made:

- The ER-DSR test has been found to be the best alternative of the elastic recovery test using ductility bath (AASHTO T 301). A very good correlation was found between these two parameters. The ER-DSR values of 40%, 50%, and 60% were representatives of 70%, 80%, and 90% ER values, respectively.
- Good correlations between AASHTO T 301 and MSCR test parameters were obtained. The MSCR percent recovery (%R) at 3.2 kPa showed a relatively better correlation with the elastic recovery test. On the other hand, the non-recoverable creep compliance (J<sub>nr</sub>) also showed a good correlation with the ER. However, the J<sub>nr</sub> value was very low for binders with a very high elastic recovery.
- The correlation between the ER-DSR and the percent recovery (%R) at 3.2 kPa from the MSCR test was developed. A good correlation was observed between these two parameters. Thus, there is a good possibility of the ER-DSR test to indicate the rutting resistance of the asphalt binder.
- Very poor correlations were observed between binder's yield energy and strain at peak stress with ER or ER-DSR test results. Thus, the BYET is not recommended. For the same reason, LAS test is not recommended either.
- The presence of the elastomer can be identified by ER-DSR and MSCR tests, but the presence of PPA cannot be determined by these test methods. Also, these test methods are not capable of characterizing PG Plus binders modified with PPA. Thus, chemical tests need to be explored to find an alternative of ER test for acid modified binders.
- The pH measurements of tested binder samples were useful to compare the acidity level of the binder and to observe any change in the pH in the binder due to its modification. Moreover, this test may enable the researchers to make a quick comparison of stiffness for multiple binder samples. Though pH measurement is not the best way to know about the asphalt chemistry, it is helpful to trace the presence of acid and degree of modification.
- The SARA analysis is useful to characterize asphalt binders based on chemical composition. As the binder properties largely depend on chemical composition, this test can be useful to predict binder parameters like rutting, fatigue. Moreover, this test is useful to observe the change in chemical composition due to aging which may eventually help to predict mechanical performance on field condition.
- Spectroscopic analysis (FTIR) can quickly detect the presence of change in quantities of functional groups that might have occurred due to any modification or aging. Therefore, FTIR test can be used as a quick tool to observe changes in chemical fingerprint due to aging.



#### Recommendations for Future Studies:

- Mastic samples can be evaluated by ER-DSR to establish a strong recommendation.
- Previous researchers found significant correlations among mechanical properties and asphalt chemistry. Therefore, further study of FTIR tests on asphalt binder samples may lead to the establishment of an efficient test protocol to evaluate the change in mechanical properties.
- Only asphalt binders are tested in the laboratory. Asphalt mixture tests along with field performance tests are recommended to get a better understanding of in-service performance.

## REFERENCES

1. Becker, Y., M.P. Mendez, and Y. Rodriguez. A Polymer Modified Asphalt. *Vision Technol*, 2001. 9:39-50.
2. Yildirim, Y. Polymer Modified Asphalt Binders. *Construction and Building Materials*, 2007. 21(1), 66-72. DOI: 10.1016/j.conbuildmat.2005.07.007.
3. Clopotel, C.S., and Bahia, H. Importance of Elastic Recovery in the DSR for Binders and Mastics. *Engineering Journal*, 2012. 16(4):99-106.
4. Lyngdal, E.T. Critical Analysis of pH and PG+ Asphalt Binder Test Methods. Master's Thesis, University of Wisconsin, Madison, 2011.
5. D'Angelo, J. Superpave Plus Binder Specifications: Why do we have them. *2<sup>nd</sup> International Symposium on Binder Rheology*, 2001.
6. Yusuf, M., Nolan, A. Eric, D. Zorn, S. Batten, E. and Shirodkar, P. Correlation between Multiple Stress Creep and Recovery (MSCR) Results and Polymer Modification of Binder. *Department of Transportation Bureau of Research*, New Jersey, 2013.
7. Clopotel, C., Mahmoud E., and Bahia. H. Modification of the Elastic Binder Recovery Test and its Relationship to Performance Related Properties of Modified Asphalt Binders. *Transportation Research Board*, Washington, D.C., 2010.
8. Tosh, D.J. and Morin, R. Building Seals and Sealants, *American Society for Testing Materials*, 1976.
9. Moraes, R., Swiertz, D., and Bahia, H. Comparison of New Test Methods and New Specifications for Rutting Resistance and Elasticity of Modified Binders. *Canadian Technical Asphalt Association*, 2017.
10. D'Angelo, J. New High-Temperature Binder Specification Using Multistress Creep and Recovery. Transportation Research Circular EC-147, *Transportation Research Board, National Research Council, National Academies*, Washington, D.C., 2010. 1-13.
11. Bukowski, J., Youtcheff, J., and Harman, T. The Multiple Stress Creep Recovery (MSCR) Procedure. *Federal Highway Administration*, 2011.
12. Hanz, A. MSCR Implementation and Impacts on Asphalt Binder Grading. *Presentation at MAPA Contractors' workshop*, Minneapolis, 2015.
13. Tabatabaee, H., Clopotel, C., Arshadi, A., and Bahia, H. Critical Problems with Using the Asphalt Ductility Test as a Performance Index for Modified Binders. *Transportation Research Board*, Washington, D.C., 2013.

14. Johnson, C.M., Wen, H., and Bahia, H. Practical Application of Viscoelastic Continuum Damage Theory to Asphalt Binder Fatigue Characterization. *Journal of Asphalt Paving Technol.*, 2009. 78:597-638.
15. Wen, H., and Bhusal, S. Toward the Development of a New Thermal Cracking Test Using the Dynamic Shear Rheometer. *Journal of Testing and Evaluation*, 2013. 41(3):1-8.
16. Johnson, C.M. Estimating Asphalt Binder Fatigue Resistance Using an Accelerated Test Method. Ph.D. Dissertation, University of Wisconsin-Madison, Madison, WI, 2010.
17. Hintz, C. Understanding Mechanisms Leading to Asphalt Binder Fatigue. Ph.D. Dissertation, University of Wisconsin, Madison, 2012.
18. Wang, J., Qin, Y., Huang, S., and Xu, J. Laboratory Evaluation of Aging Behaviour of SBS Modified Asphalt. *Advances in Materials Science and Engineering*, 2017. Article ID 3154634, 12 pages, <https://doi.org/10.1155/2017/3154634>.
19. Sultana S. and Bhasin, A. Effect of Chemical Composition on Rheology and Mechanical Properties of Asphalt Binder. *Construction and Building materials*, October 2014.
20. Weigel S., and Stephan, D. Relationships Between the Chemistry and the Physical Properties of Bitumen. *Road Materials and Pavement Design*, 2017. <https://doi.org/10.1080/14680629.2017.1338189>.
21. Alam, S., Hossain, Z., and Baumgardner, G. Linking Chemical Compositions and Rheological Properties of Asphalt Binders. *Transportation Research Board*, Washington D.C., 2018.
22. Paliukaite, M.V. Evaluation of Bitumen Fractional Composition Depending on the Crude Oil Type and Production Technology. *Environmental Engineering. Proceedings of the International Conference on Environmental Engineering. ICEE. 9, p. 1*. Vilnius Gediminas Technical University, Department of Construction Economics and Property, 2014.
23. Catherine, B., and Heinerwadel, R. Fourier Transform Infrared (FTIR) Spectroscopy. *R. Photosynth Res*, (2009). 101: 157, <https://doi.org/10.1007/s11120-009-9439-x>.
24. Lamontagne, J., Dumas, P., Mouillet, V., and Kister, J. Comparison by Fourier Transform Infrared (FTIR) Spectroscopy of Different Ageing Techniques: Application to Road Bitumens. *Fuel*, 2001. 80(4), 483-488.
25. Nasrekani A.A., M. Nakhaei, K. Naderi, M. Taher Abu-Lebdeh, E.H. Fini, and S. Aflaki. Gilsonite Modified Asphalt for Use in Pavement Construction. *American Journal of Engineering and Applied Sciences*, 2018. Volume 11, Issue 2, Pages 444-454, DOI : 10.3844/ajeassp.2018.444.454.
26. Fini, E.H., E.W. Kalberer, A. Shahbazi, M. Basti, Z. You, H. Ozer, and Q. Aurangzeb. Chemical Characterization of Biobinder from Swine Manure: Sustainable Modifier for Asphalt Binder. *Journal of Materials in Civil Engineering*, November 2011. Volume 23 Issue 11.

27. Yao H., Z. You, L. Li, S.W. Goh, C.H. Lee, Y.K. Yap, and X. Shi. Rheological Properties and Chemical Analysis of Nanoclay and Carbon Microfiber Modified Asphalt with Fourier Transform Infrared Spectroscopy. *Construction and Building Materials*, 2013. Volume 38, Pages 327-337, ISSN 0950-0618, <https://doi.org/10.1016/j.conbuildmat.2012.08.004>.
28. Modified Asphalt Research Center. Measuring Asphalt Binder Yield Energy and Elastic Recovery Using the Dynamic Shear Rheometer, Madison.
29. Bahia, H.U., D.I. Hanson, M. Zeng, H. Zhai, M.A. Khatri, and M.R. Anderson. A Project NCHRP 9-10 Superpave Protocols for Modified Asphalt Binders. Draft Topical Report (Task 9), *Prepared for National Cooperative Highway Research Program*, Transportation Research Board, National Research Council, Washington, D.C., 2000.
30. Bahia, H.U., H. Zhai, M. Zeng, Y. Hu, and Turner. Development of Binder Specification Parameters Based on Characterization of Damage Behavior. *Journal of the Association of Asphalt Paving Technologists*, Louisville, Kentucky, 2001. Vol. 70, pp. 442-470.
31. Anderson, M., J. D'Angelo, and D. Walker. MSCR: A Better Tool for Characterizing High-Temperature Performance Properties. *Asphalt*, 2010. 25(2).
32. Colthup, N.B., L.H. Daly, and S.E. Wiberly. *Introduction to infrared and Raman spectroscopy*. Academic Press, New York, 1975.
33. Griffith, P.R., J.A. De Haseth. *Fourier Transform Infrared Spectroscopy*. Wiley, New York, 1986.
34. Robertson, R.E., J.F. Branthaver, P.M. Harnsberger, J.C. Peterson, S.M. Dorrence, J.F. McKay, and J.E. Tauer. Fundamental Properties of Asphalts and Modified Asphalts, 2001 volume I: Interpretive report (No. FHWA-RD-99-212).
35. Hassan, M.N., Z. Hossain, and G. Baumgardner. Quantification of Effects of Nanoclays on Chemical Compositions and Selected Mechanical Properties of Asphalt Binder and Aggregate Systems. *Transportation Research Board 98<sup>th</sup> Annual Meeting*, Washington D.C., 2019.
36. Zhang, F., J. Yu, and J. Han. Effects of Thermal Oxidative Ageing on Dynamic Viscosity, TG/DTG, DTA and FTIR of SBS- and SBS/Sulfur-modified Asphalts. *Construction and Building Materials*, 2011.25(1):129–37.
37. Branco, V.A.M., G.A. Mansoori, L.C.D.A. Xavier, S.J. Park, and H. Manafi. Asphaltene Flocculation and Collapse from Petroleum Fluids. *J Petrol Sci Eng*, 2001. 32(2–4):217–30.

## APPENDIX A: CHEMICAL TEST RESULTS

Table A1. pH results.

Sample	pH
S1B1	8.3
S1B2	4.8
S1B3	6.9
S1B4	2.8
S2B1	6.2
S2B2	2.8
S2B3	5.9
S2B4	2.8

Table A2. SARA fractions for unaged binders.

Sample	Saturates	Aromatics	Resin	Asphaltenes	% Recovered
S1B1	10	38.3	31.8	19.9	
S1B2	9.6	41.6	27.3	21.5	96.5
S1B3	8.9	41	30.2	19.9	93
S1B4	9.5	35	34	21.5	90.8
S2B1	6.8	43.6	36.3	13.2	98
S2B2	7.4	45.8	28	18.8	99
S2B3	5	35.4	42.3	17.3	94.7
S2B4	5.6	34.8	40.2	19.4	98.7

Table A3. SARA fractions for RTFO-aged binders.

Sample	Saturates	Aromatics	Resin	Asphaltenes	% Recovered
S1B1	7.9	41.4	29.3	21.4	
S1B2	6.3	37.9	31.6	24.3	96.5
S1B3	9.3	32.3	34.1	24.3	93
S1B4	6.4	38.8	31.5	23.3	90.8
S2B1	6.3	43	33.5	17.2	98
S2B2	5.6	40.8	33	20.6	99
S2B3	6.6	39.2	33	21.2	94.7
S2B4	6.9	39.6	30.7	22.8	98.7

**Table A4. SARA fractions for PAV-aged binders.**

<b>Sample</b>	<b>Saturates</b>	<b>Aromatics</b>	<b>Resin</b>	<b>Asphaltenes</b>	<b>% Recovered</b>
S1B1	9.5	31.6	32.4	26.4	
S1B2	8.4	33	30	28.6	96.5
S1B3	8.4	29.9	32.5	29.2	93
S1B4	8.2	31.8	24.9	35.2	90.8
S2B1	5.3	39.1	35.7	19.8	98
S2B2	7.1	39.8	28.2	24.9	99
S2B3	6.4	37.6	30.4	25.6	94.7
S2B4	6.6	33.8	30	29.6	98.7

**Table A5 Gasetel Index (I<sub>c</sub>).**

<b>Sample</b>	<b>Colloidal Stability</b>
S1B1	0.43
S1B2	0.45
S1B3	0.4
S1B4	0.45
S2B1	0.25
S2B2	0.35
S2B3	0.29
S2B4	0.33

## APPENDIX B: MECHANICAL TEST RESULTS

Table B1. ER-DSR test results for unaged binders.

Sample Name	Modifier	Performance Grade	Average Values	St Dv.	Cov.
S1B1		PG 64-22	8.95	0.46	5.09%
S1B2	PPA	PG 70-22	14.39	0.13	0.88%
S1B3	SBS	PG 70-22	53.12	0.51	0.97%
S1B4	PPA+SBS	PG 76-22	65.00	1.69	2.59%
S2B1		PG 64-22	9.97	0.75	7.47%
S2B2	PPA	PG 70-22	17.71	0.91	5.16%
S2B3	SBS	PG 70-22	55.49	1.15	2.07%
S2B4	PPA+SBS	PG 76-22	64.66	1	1.55%

Table B2. ER-DSR test results for RTFO-aged binders.

Sample Name	Modifier	Performance Grade	Average	St Dv.	Cov.
S1B1	None	PG 64-22	21.50	0.60	2.81%
S1B2	PPA	PG 70-22	20.31	0.64	3.13%
S1B3	SBS	PG 70-22	57.32	0.54	0.94%
S1B4	PPA+SBS	PG 76-22	65.39	1.00	1.52%
S2B1	None	PG 64-22	15.26	0.08	0.51%
S2B2	PPA	PG 70-22	21.63	0.14	0.66%
S2B3	SBS	PG 70-22	52.16	0.60	1.14%
S2B4	PPA+SBS	PG 76-22	62.00	1.14745	1.85%

**Table B3. ER-DSR test results for additional binders (unaged binders).**

<b>Source</b>	<b>Grade</b>	<b>Name</b>	<b>Average</b>	<b>St Dv.</b>	<b>Cov.</b>
Source C	PG 70-22	S3B3	48.00	2.65	5.52%
Source C	PG 76-22	S3B4	78.38	2.92	3.73%
Source D	PG 70-22	S4B3	53.85	0.18	0.33%
Source D	PG 76-22	S4B4	71.86	0.36	0.50%
Source E	PG 70-22	S5B3	38.55	0.38	0.99%
Source E	PG 76-22	S5B4	60.11	1.50	2.49%
Source F	PG 70-22	S6B3	61.25	0.04	0.06%
Source F	PG 76-22	S6B4	69.33	11.44	16.50%
Source G	PG 70-22	S7B3	43.92	0.83	1.88%
Source G	PG 76-22	S7B4	66.49	0.30	0.45%
Source H	PG 70-22	S8B3	63.29	0.37	0.58%
Source H	PG 76-22	S8B4	76.77	0.94	1.23%
Source I	PG 70-22	S9B3	55.67	1.08	1.94%
Source I	PG 76-22	S9B4	65.60	0.80	1.22%
Source J	PG 70-22	S10B3	73.80	0.52	0.70%
Source J	PG 76-22	S10B4	60.88	1.48	2.44%

**Table B4. ER-DSR test results for additional binders (RTFO-aged binders).**

<b>Source</b>	<b>Grade</b>	<b>Name</b>	<b>Average</b>	<b>St Dv.</b>	<b>Cov.</b>
Source C	PG 70-22	S3B3	48.00	2.65	5.52%
Source C	PG 76-22	S3B4	78.38	2.92	3.73%
Source D	PG 70-22	S4B3	53.85	0.18	0.33%
Source D	PG 76-22	S4B4	71.86	0.36	0.50%
Source E	PG 70-22	S5B3	38.55	0.38	0.99%
Source E	PG 76-22	S5B4	60.11	1.50	2.49%
Source F	PG 70-22	S6B3	61.25	0.04	0.06%
Source F	PG 76-22	S6B4	69.33	11.44	16.50%
Source G	PG 70-22	S7B3	43.92	0.83	1.88%
Source G	PG 76-22	S7B4	66.49	0.30	0.45%
Source H	PG 70-22	S8B3	63.29	0.37	0.58%
Source H	PG 76-22	S8B4	76.77	0.94	1.23%
Source I	PG 70-22	S9B3	55.67	1.08	1.94%
Source I	PG 76-22	S9B4	65.60	0.80	1.22%
Source J	PG 70-22	S10B3	73.80	0.52	0.70%
Source J	PG 76-22	S10B4	60.88	1.48	2.44%



**Table B5. Binder tests result summary.**

<b>Sample</b>	<b>%R</b>	<b>ER-DSR (Unaged)</b>	<b>ER-DSR (RTFO)</b>	<b>BYET</b>	<b>ER</b>	<b>Jnr</b>	<b>Nf at 2.5% Strain</b>	<b>Nf at 5% Strain</b>	<b>Strain at peak stress</b>
S1B1	1.99	8.95	21.50	157.24	-	2.07	12707	1111	203.6
S1B2	11.21	14.39	20.31	75.9	-	1.03	13911	1217	208.78
S1B3	29.51	53.12	57.32	1190.65	70	0.64	13675	1196	1790.65
S1B4	30.82	65.00	65.39	1598.95	80	0.32	11502	1006	1550.21
S2B1	1.4	9.97	15.26	125.88	-	1.98	11887	1040	215.07
S2B2	4.06	17.71	21.63	120.46	-	1.86	14249	1247	181.74
S2B3	27.32	55.49	52.16	1274.61	68	0.8	13128	1120	2033.39
S2B4	29.41	64.66	62.00	1581.79	80	0.35	12384	1083	1606.33
S3B3	23.65	48.00	65.61	907.22	71	0.55	-	-	1372.45
S3B4	45.65	78.38	79.15	3363.51	89	0.25	-	-	3071.87
S4B3	44.28	53.85	54.81	1059.42	69	0.65	-	-	2469.87
S4B4	77.09	71.86	69.84	1936.52	85	0.18	-	-	1976.41
S5B3	28.11	38.55	46.16	528.09	65	0.79	-	-	1205.54
S5B4	75.28	60.11	65.25	911.31	83	0.17	-	-	1197.68
S6B3	75.61	61.25	61.59	632.86	78	0.16	-	-	942.75
S6B4	91.97	69.33	76.53	1608.82	93	0.04	-	-	1340.81
S7B3	37.03	43.92	52.15	704.92	72	0.67	-	-	1604.31
S7B4	74.75	66.49	71.01	1404.31	92	0.15	-	-	1540.87
S8B3	74.07	63.29	63.69	554.11	81	0.21	-	-	1008.04
S8B4	92.15	76.77	77.56	-	95	0.04	-	-	-
S9B3	63.45	55.67	-	-	82	0.35	-	-	-
S9B4	85.73	65.60	-	-	84	0.09	-	-	-
S10B3	79.73	73.80	-	-	90	0.16	-	-	-
S10B4	69.39	60.88	-	-	95	0.22	-	-	-

# APPENDIX C: FTIR TEST RESULTS

## C.1. FTIR Spectra for Asphalt Binder Sample

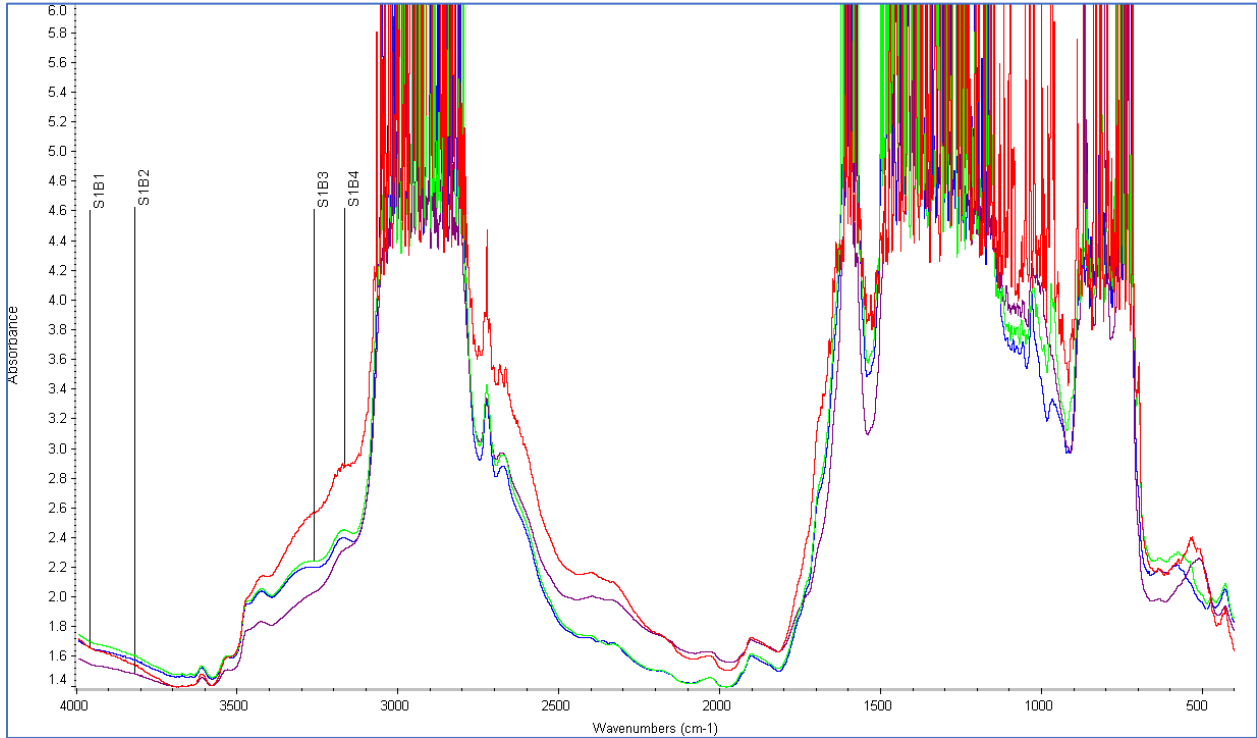


Figure C1. FTIR spectra for S1 (unaged) binder sample.

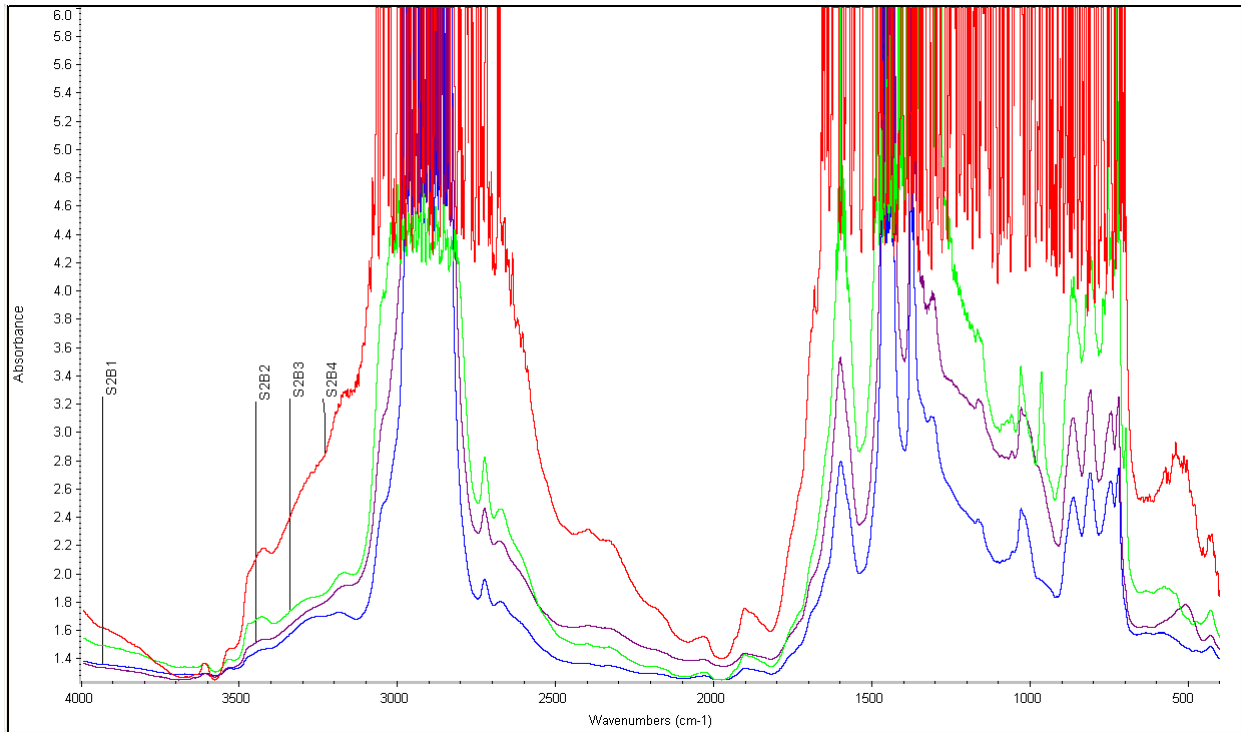


Figure C2. FTIR spectra for S2 (unaged) binder sample.

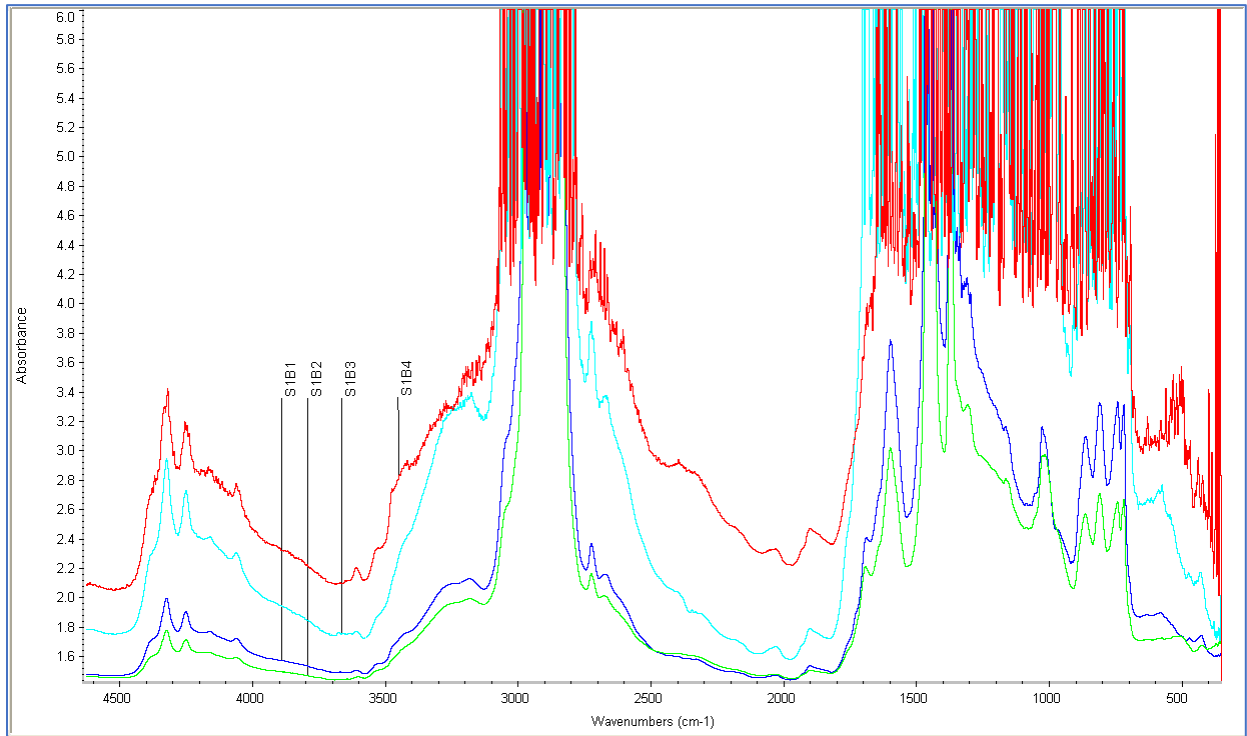


Figure C3. FTIR spectra for S1 (RTFO-aged) binder sample.

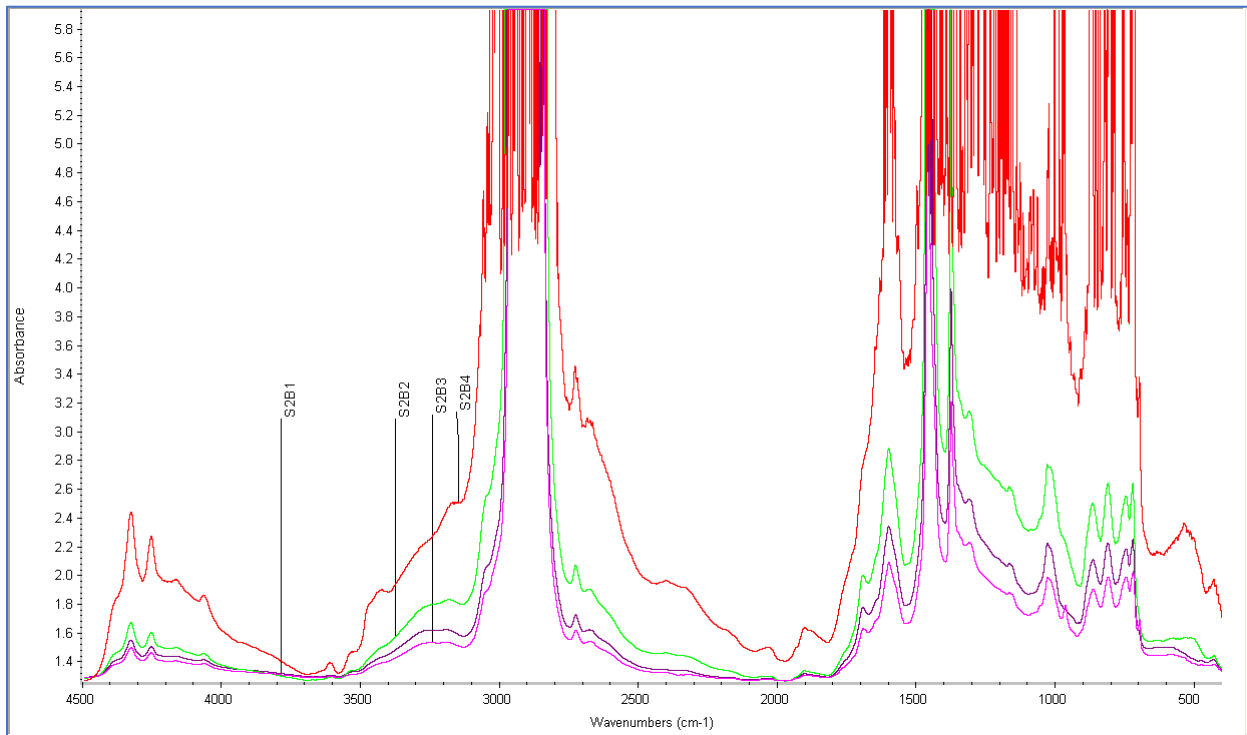


Figure C4. FTIR spectra for S2 (RTFO-aged) binder sample.

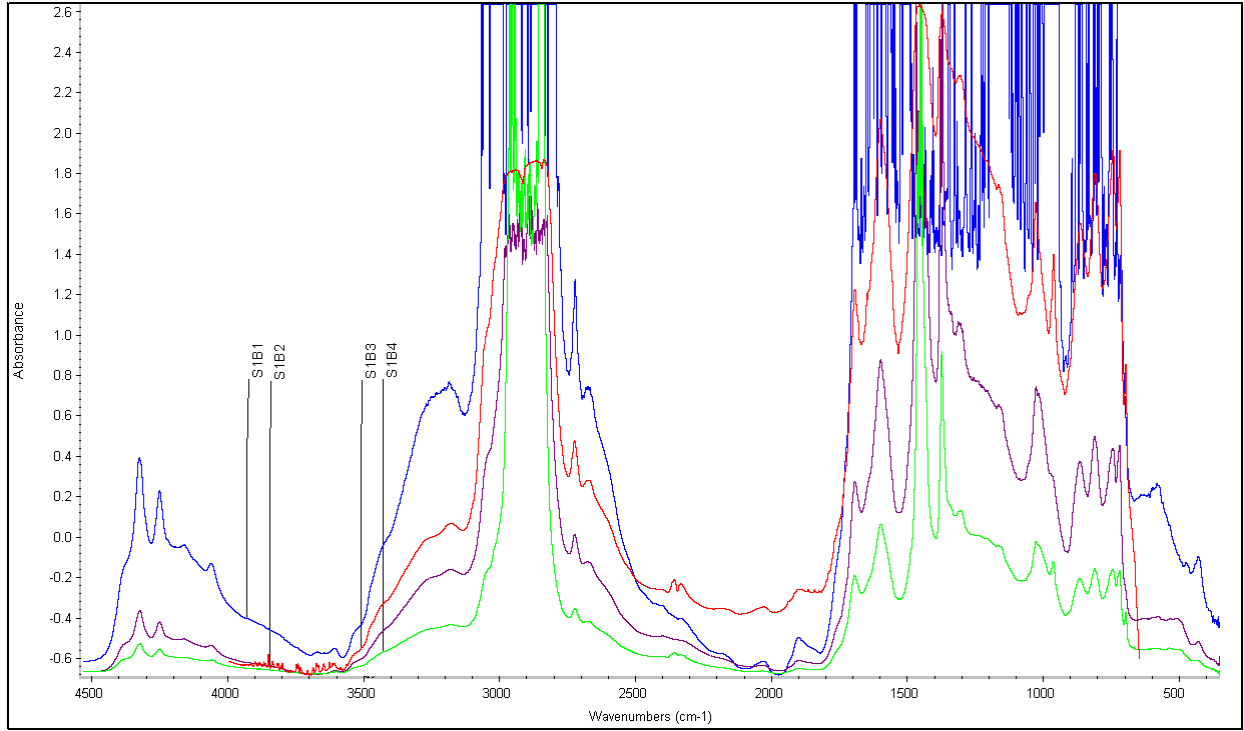


Figure C5. FTIR spectra for S1 (PAV-aged) binder sample.

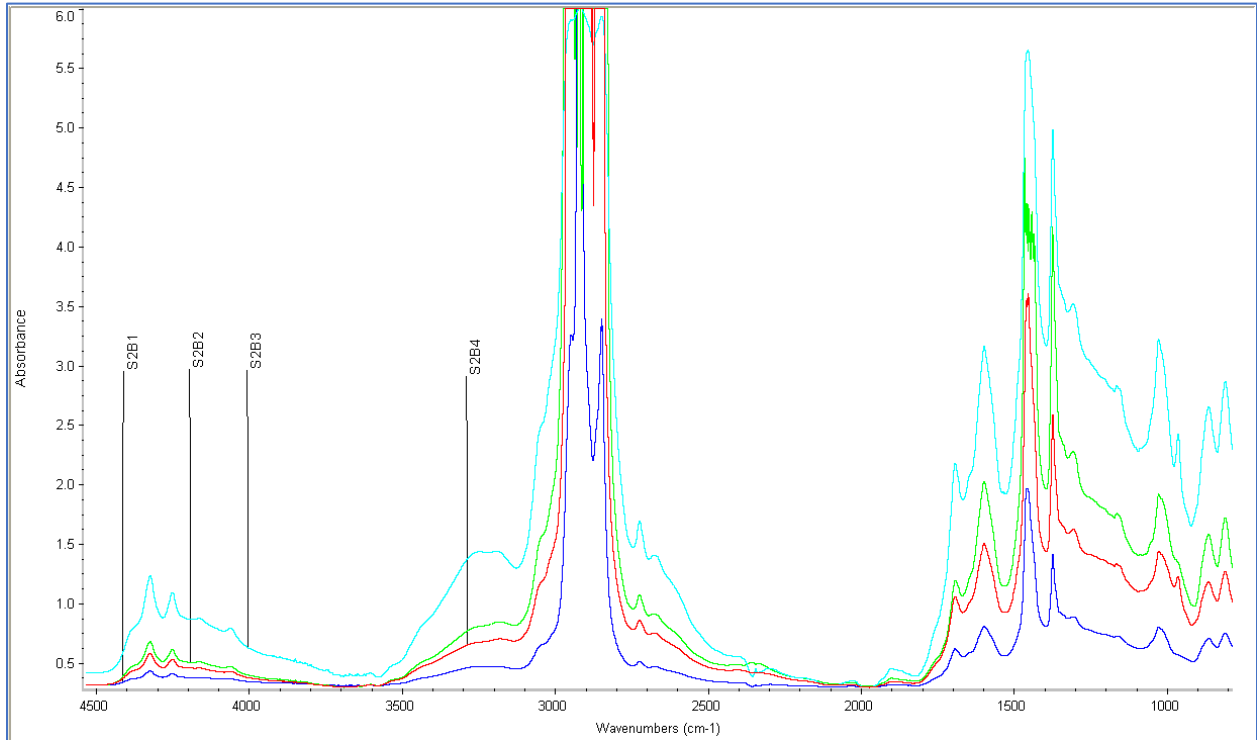


Figure C6. FTIR spectra for S2 (PAV-aged) binder sample.

**Table C1. Ratio of bonding for source 1 (unaged) binders.**

Ratio of Bonding	HC=CH	S=O	C-H of CH <sub>3</sub>	C-H of - (CH <sub>2</sub> ) <sub>n</sub> -	C=C	C=O
Wave Number (cm <sup>-1</sup> )	966	1030	1376	1460	1600	1690
S1B1	0.0003	0.004	0	0	0.0122	0
S1B2	0	0.0003	0.0118	0.0055	0.0372	0
S1B3	0.0004	0.0005	0.0001	0	0.003	0.0006
S1B4	0.0016	0.0003	0.0111	0.0058	0.018	0

**Table C2. Ratio of bonding for source 2 (unaged) binders.**

Ratio of Bonding	HC=CH	S=O	C-H of CH <sub>3</sub>	C-H of - (CH <sub>2</sub> ) <sub>n</sub> -	C=C	C=O
Wave Number (cm <sup>-1</sup> )	966	1030	1376	1460	1600	1690
S2B1	0.0014	0.0026	0.0002	0.0169	0.0309	0
S2B2	0.006	0.0004	0.0017	0.0011	0.0228	0.0003
S2B3	0.0034	0.0033	0	0	0.0007	0.0002
S2B4	0.0011	0.0005	0.0081	0.0298	0.013	0

**Table C3. Ratio of bonding for source 1 (RTFO-aged) binders.**

Ratio of Bonding	HC=CH	S=O	C-H of CH <sub>3</sub>	C-H of - (CH <sub>2</sub> ) <sub>n</sub> -	C=C	C=O
Wave Number (cm <sup>-1</sup> )	966	1030	1376	1460	1600	1690
S1B1	0	0.0151	0.0242	0	0.0221	0.0016
S1B2	0.0004	0.0194	0.0241	0.0705	0.0192	0.0025
S1B3	0.0013	0.0095	0	0.0009	0.018	0.0024
S1B4	0.0011	0.0018	0.0186	0.0454	0.0028	0

**Table C4. Ratio of bonding for source 2 (RTFO-aged) binders.**

Ratio of Bonding	HC=CH	S=O	C-H of CH <sub>3</sub>	C-H of - (CH <sub>2</sub> ) <sub>n</sub> -	C=C	C=O
Wave Number (cm <sup>-1</sup> )	966	1030	1376	1460	1600	1690
S2B1	0	0.0114	0.0144	0.0013	0.0162	0.0019
S2B2	0.0004	0.0155	0.0005	0.0191	0.0154	0.0016
S2B3	0.0011	0.0074	0.0124	0.0175	0.0149	0.0005
S2B4	0.0007	0.0014	0.0061	0.0164	0.0054	0

**Table C5. Ratio of bonding for source 1 (PAV-aged) binders.**

Ratio of Bonding	HC=CH	S=O	C-H of CH <sub>3</sub>	C-H of - (CH <sub>2</sub> ) <sub>n</sub> -	C=C	C=O
Wave Number (cm <sup>-1</sup> )	966	1030	1376	1460	1600	1690
S1B1	0.0002	0.0019	0.0043	0.0147	0.0049	0.0045
S1B2	0.0007	0.0199	0.0018	0.0001	0.02	0.0047
S1B3	0.0021	0.0035	0.0051	0.2	0.0155	0.0033
S1B4	0.0014	0.0056	0.0126	0.0005	0.0156	0.0041

**Table C6. Ratio of bonding for source 2 (PAV-aged) binders.**

<b>Ratio of Bonding</b>	<b>HC=CH</b>	<b>S=O</b>	<b>C-H of CH<sub>3</sub></b>	<b>C-H of - (CH<sub>2</sub>)<sub>n</sub>-</b>	<b>C=C</b>	<b>C=O</b>
Wave Number (cm <sup>-1</sup> )	966	1030	1376	1460	1600	1690
S2B1	0	0.0025	0.0022	0.0095	0.0027	0.0007
S2B2	0.0005	0.0148	0.014	0.0001	0.0173	0.0025
S2B3	0.0012	0.0108	0.0091	0.0359	0.0169	0.0043
S2B4	0.0012	0.0061	0.0096	0.041	0.0143	0.0034